



Bruce R. White and Associates
3207 Shelter Cove Avenue
Davis, California 95616-2627
(530) 758-1496

FINAL REPORT

**A WIND-TUNNEL STUDY OF WIND SPEEDS FOR THE
RENOVATION OF HAYWARD FIELD**

Bruce R. White, Principal

Scott Brisbin, Engineer

Bethany Kuspa, Engineer

***Prepared for:
IDC Architects
2020 SW Fourth Ave, Third Floor
Portland, OR 97201***

February 2007

STATEMENT OF LIMITATION AND DISCLAIMER

"The professional opinions and judgments set forth in this report are based on laboratory testing performed pursuant to acceptable wind engineering standards. All the laboratory test results are limited to the specific conditions of the applicable testing program. I believe my observations and interpretations of the test results conform to current applicable engineering techniques and principles. No warranty is expressed or implied."

Table of Contents

EXECUTIVE OVERVIEW	2
1. INTRODUCTION	3
2. WIND-TUNNEL MODEL	3
3. METHODOLOGY	6
CONVERTING WIND-TUNNEL DATA TO FULL-SCALE ESTIMATES	7
4. WIND-TUNNEL MEASUREMENTS	8
5. RESULTS	9
SUMMARY OF RESULTS FOR WIND FROM THE NORTH	10
SUMMARY OF RESULTS FOR WIND FROM THE NORTHEAST	10
SUMMARY OF RESULTS FOR WIND FROM THE NORTHWEST	11
GRAPHIC RESULTS	11
WIND-TUNNEL PROFILE RESULTS	24
PEDESTRIAN RESULTS	24
6. MITIGATION SUGGESTIONS	26
7. CONCLUDING REMARKS	26
8. REFERENCES	28
APPENDIX A	29
WIND-TUNNEL RESULTS	
APPENDIX B	37
THE ATMOSPHERIC BOUNDARY LAYER WIND TUNNEL	
APPENDIX C	39
WIND-TUNNEL ATMOSPHERIC FLOW SIMILARITY PARAMETERS	
APPENDIX D	43
WIND-TUNNEL ATMOSPHERIC BOUNDARY-LAYER SIMILARITY	

EXECUTIVE OVERVIEW

A wind-tunnel study of the pedestrian-level wind environment was conducted for the proposed Hayward Field renovation project. The wind study used a 1:240 scaled model (one-inch on the wind-tunnel model equals 20 feet in full scale) of the Hayward Field site and surrounding area. Tests were conducted for three wind directions: north, northeast and northwest. A reference wind speed of 7.5 meters per second at a height of 10 meters above ground level was used to analyze the results.

The main objective of the test was to predict the wind speeds that would exist on the site for various orientations of the proposed pylon structures' wind screens. Wind data over one hundred and twenty-two surface points was taken to evaluate the performance of the pylons. Using the test data as input to a computer code analysis, full-scale wind speeds were estimated based on the wind-tunnel data. Nineteen of the measurement locations represented pedestrian areas along both Fifth and Agate Streets, including the entrance area to Hayward Field at the northeast corner.

It was desired that wind speeds at 5-feet (1.5 meters) above ground level be below 4.5 miles per hour (2 meters per second) on the field. First, the model was tested in the wind tunnel without any pylons present to provide a baseline case. Next, the pylons were placed on the model and tested at three specific settings. For the first setting, the pylons' wind screens were set perpendicular to the oncoming wind; the second setting positioned the screens at a 75-degree angle counterclockwise to the oncoming wind (as viewed from above); the third setting positioned the screens such that the angle between them and the oncoming wind was 60 counterclockwise to the oncoming wind.

1. INTRODUCTION

This report describes the methodology developed to address pedestrian-level winds in and around the Hayward Field renovation wind-tunnel study. The assessment is accomplished through wind-tunnel testing that couples full-scale meteorological data to physical modeling data. The primary application of this evaluation process is in the environmental impact assessment of proposed pylons that may substantially alter pedestrian-level winds in site areas.

2. WIND-TUNNEL MODEL

A 1:240 scaled model (one inch on the wind-tunnel model equals twenty feet full scale) was provided by IDC Architects at the beginning of the project. The model was centered about the center of the field. Areas beyond the field were also built and simulated in the wind tunnel for each wind direction that was tested. Winds speeds and turbulence intensities were measured at 122 representative locations in the test of the project for the three prevailing wind directions of north, northeast and northwest. Figure 1 shows an overhead photograph of the wind-tunnel model in the wind tunnel. Figure 2 illustrates the measurement locations on the model along with screen identification and points for which profiles were taken.

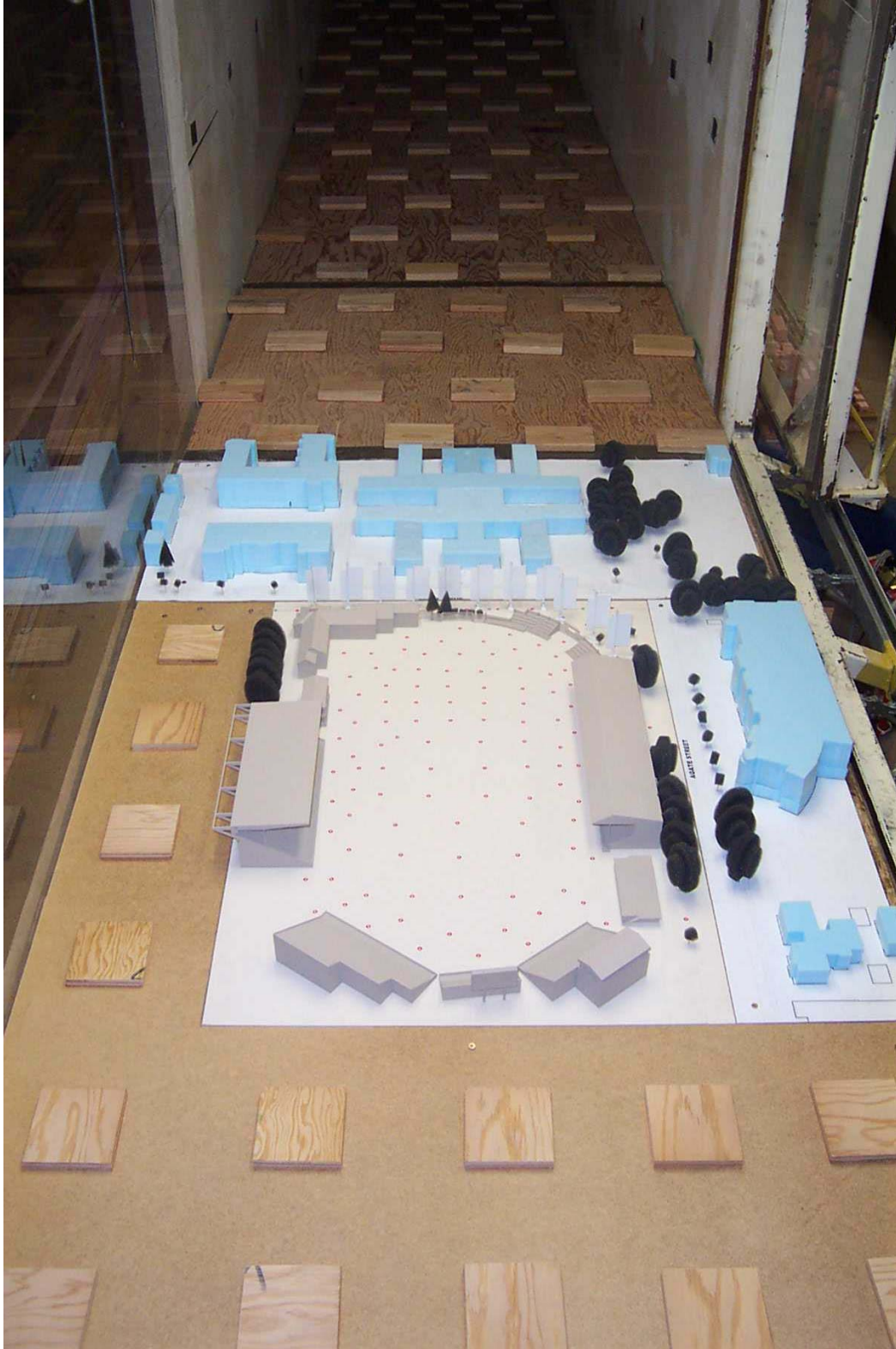


Figure 1. Wind-tunnel model in wind tunnel, simulating a north wind with the eleven pylons (screens) at 90 degrees to oncoming wind.

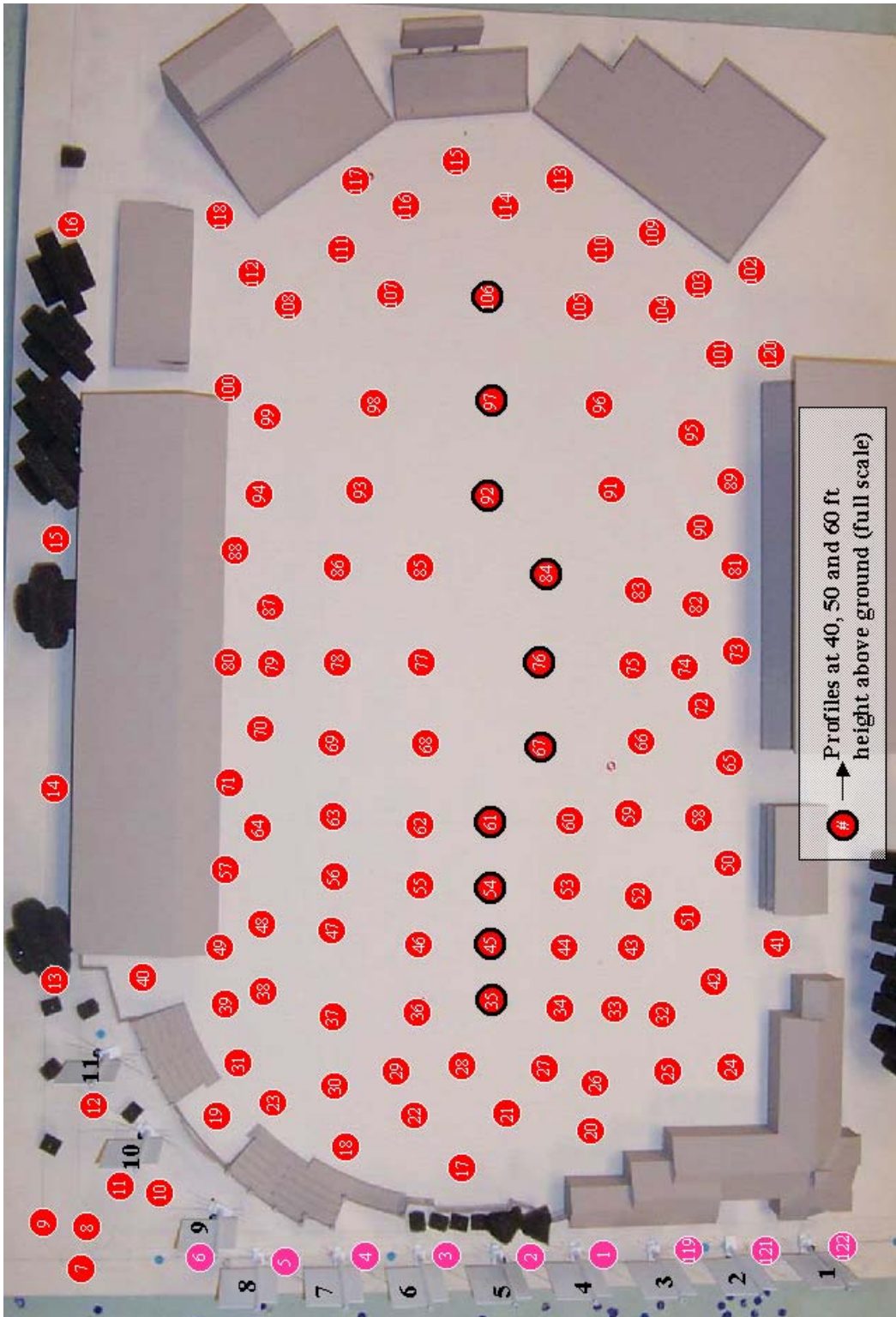


Figure 2. Measurement locations on wind-tunnel model, note north is down.

3. METHODOLOGY

For each surface wind-speed measurement made in the wind tunnel, it is desirable to estimate an associated full-scale wind speed. The determination of the full-scale wind speeds will depend upon the nature of the meteorological conditions at the site. For the present study, it was requested to use the full-scale mean wind speed of 16.8 miles per hour (7.5 meters per second) obtained at a height of 32.8 feet (10 meters) above the ground as an approach wind speed and profile (with a power law coefficient of about 0.2, consistent with computational modeling input). All wind data was reduced using this constraint. It was desired that the wind speeds on the field not exceed a benchmark of 4.5 miles per hour (2 meters per second).

For the present case, the equivalent full-scale pedestrian-level wind speed is determined from wind-tunnel measurements made for the three wind directions. The process of obtaining full-scale wind speeds from wind-tunnel data involves several steps. First, the ratio of the reference height wind speed to the wind speed at pedestrian-level is calculated from the results of the wind-tunnel experiment for each major direction at each observation location. The wind-tunnel ratios are used to scale wind-tunnel speeds to the full-scale speeds by use of the power-law relationship given by Davenport (1961). Roughness elements upwind of the model in the wind tunnel were arranged to obtain a profile with an α of 0.2. For the current study, a full-scale reference speed of 16.8 miles per hour (7.5 meters per second) at a height of 32.8 feet (10 meters) was used in the power-law calculations.

Four separate settings were tested for each wind direction. First, the model was tested in the wind tunnel without any pylons present to provide a baseline case. Next, the pylons were placed on the model and tested at three specific settings. For the first setting, all the pylons' wind screens were set perpendicular to the oncoming wind; the second setting positioned all the screens at a 75-degree angle counterclockwise to the oncoming wind (as viewed from above); the third setting positioned all the screens such that the angle between them and the oncoming wind was 60 counterclockwise to the oncoming wind.

CONVERTING WIND-TUNNEL DATA TO FULL-SCALE ESTIMATES

The process of converting wind-tunnel data to full-scale wind-speed estimates involves several steps. After the raw data is reduced into R-values, full-scale wind speeds are estimated for each wind direction, assuming a reference wind speed of 16.8 mile per hour (7.5 meter per second) wind at a height of 32.8 feet (10 meters) above the ground. An R-value is the ratio of wind speed measured at pedestrian level divided by the free stream wind speed, both as measured in the wind tunnel. All calculations were done using an Excel[®] spreadsheet. The definitions below are used to describe the variables used in the following equations (Kuspa 2006):

- $R_{\text{direction}}$ = the R-value of one point for the specified wind direction; for example, R_{NW} is the R-value of a single point for the northwest wind direction.
- U_{point} = the wind speed at the point.
- U_{ref} = the reference wind speed, which is 16.8 miles per hour (7.5 meters per second).
- U_{∞} = free stream wind speed in the wind tunnel.
- $U_{\text{geostropic}}$ = the geostropic wind speed.
- z_{ref} = the height corresponding to U_{ref} , which for full-scale is 32.8 feet (10 meters).
- z_{point} = the height corresponding to U_{point} .
- δ = the boundary layer height, which is about 2 feet (0.6 meters) in the wind tunnel.
- α = the power-law exponent, which is 0.2 for Hayward Field. The α simulated in the wind tunnel is 0.2, which provides a suitable simulation.
- The subscript “Wind Tunnel” refers to wind-tunnel data.
- The subscript “Full Scale” refers to full-scale values.

The power-law is used to show the relationship of full-scale wind speeds to measured wind speeds in the wind tunnel (White 1992):

$$\left(\frac{U_{\text{point}}}{U_{\text{ref}}} \right)_{\text{Full Scale}} = \left(\frac{U_{\text{point}}}{U_{\text{ref}}} \right)_{\text{Wind Tunnel}} = \left(\frac{z_{\text{point}}}{z_{\text{ref}}} \right)^{\alpha} \quad (1)$$

Rearranging the variables and multiplying and dividing by U_{∞} yields (White 1992):

$$\left(U_{\text{point}} \right)_{\text{Full Scale}} = \left(U_{\text{point}} \right)_{\text{Wind Tunnel}} \cdot \frac{\left(U_{\text{ref}} \right)_{\text{Full Scale}}}{\left(U_{\text{ref}} \right)_{\text{Wind Tunnel}}} \rightarrow \quad (2)$$

$$\left(U_{\text{point}} \right)_{\text{Full Scale}} = \left(\frac{U_{\text{point}}}{U_{\infty}} \right)_{\text{Wind Tunnel}} \cdot \left(U_{\text{ref}} \right)_{\text{Full Scale}} \cdot \left(\frac{U_{\infty}}{U_{\text{ref}}} \right)_{\text{Wind Tunnel}}$$

By definition, $(U_{\text{point}}/U_{\text{ref}})$ is the R-value. However, wind tunnel data is not accurate at the level of U_{∞} due to the Coriolis effect in full-scale (White 1992). Therefore, it is desired to have another relationship between all of these variables. Using the information for the boundary layer height, about 60 cm, the height of the reference velocity, $1000\text{cm}/240 = 4.167$ cm, and power-law exponent of 0.2 for the Hayward Field, the power-law equation yields the following (White 1992):

$$\left(\frac{U_{\infty}}{U_{\text{refc}}} \right)_{\text{Wind Tunnel}} = \left(\frac{\delta}{z_{\text{ref}}} \right)^{\alpha} = 1.7 \quad (3)$$

Substituting this finding into the above equations gives the relationship between the reference wind speed, R-value and full-scale speed at a specific point with wind from one wind direction (White 1992):

$$\left(U_{\text{point}} \right)_{\text{Full Scale}} = 1.7 \cdot R_{\text{direction}} \cdot \left(U_{\text{ref}} \right)_{\text{Full Scale}}$$

4. WIND-TUNNEL MEASUREMENTS

Wind speed and the corresponding turbulence intensity were measured using a TSI, Inc. Model 1210 single hot-wire anemometer probe. Using a Lab VIEW data-acquisition system, data was acquired and digitally recorded for each measurement point at a sample rate of 1000 Hz for 30 seconds. This yielded 30,000 individual voltage values that were individually converted to instantaneous wind speed according to a hot-wire calibration curve that was acquired before the testing commenced. The 30,000 samples were then averaged to produce a single mean surface

wind speed and a root-mean-square value for the turbulence intensity. The resulting mean speeds and turbulence intensities represent one-hour full-scale average time measurements when the wind-tunnel data is converted to the full scale time.

The majority of the testing focused on the areas directly on the field as well as other points of interest. Tests were conducted for the three wind directions: north, northeast and northwest. For each wind direction tested, the approach wind speed, as a function of height above the ground (boundary-layer velocity profile), was non-dimensionally simulated in the wind tunnel based upon the upwind surface terrain-roughness features. This technique is known to provide accurate surface wind speed simulation of the full-scale case (see Appendix B). Mean wind speeds and the fluctuating components of the speeds (i.e., turbulence intensities) were measured at 122 surface locations distributed around the Hayward Field site.

5. RESULTS

Reduced wind-tunnel data was used to create contour plots of full-scale wind speeds at ground level (Figures 3 through 14). In order to best convey the results, they are presented in two methods: a written description, through a summary by wind direction, and graphically, through the use of contour plots. All contour plots were generated using Matlab v. 7. All points within the stadium are included, which excludes the points along the northern and eastern pedestrian areas (i.e, points #1-16, #119, #121, and #122). In order to generate contour plots, a uniformly spaced grid was required. The dimensions of the grid match the full-scale dimensions of the Hayward Field architectural model, which are 520 feet (158.5 meters) east from the southwest corner and 740 feet (225.6 meters) north from the southwest corner. The node spacing was chosen to be 5 feet (1.5 meters) in either direction. The 103 non-uniformly spaced wind tunnel data points were then fit to the uniform grid via a cubic interpolation function. The result is a smooth surface that passes through all of the supplied data. The wind speeds are distinguished by a color scheme which spans from 0 to 16.8 miles per hour (7.5 meters per second). Wind speeds below 4.5 miles per hour (2 meters per second) are shown in blue.

SUMMARY OF RESULTS FOR WINDS FROM THE NORTH

- Reductions in the northwest corner area below 2 m/s are present in all orientations.
- Regardless of wind screen orientation, a jetting effect is observed at the northeast entry gate. The effect is smallest with the 90 degree orientation and largest with the 60 degree orientation.
- Gaps between the temporary seating and permanent seating at the southwest and southeast corners create additional jetting effects with wind speeds between 4 m/s and 6 m/s. This effect is minimized using the 75 degree wind screen orientation.
- The 75 degree wind screen orientation and 90 degree wind screen orientation reduce the pedestrian level wind speeds to between roughly 2 m/s and 4 m/s in the regions not mentioned. The 60 degree wind screen orientation shows reductions that are roughly 5% - 10% less compared to the other two cases. The difference is best illustrated in the southern portion of the field where wind speeds near 4.5 m/s are prevalent.

SUMMARY OF RESULTS FOR WINDS FROM THE NORTHEAST

- Reductions in the northern region below 2 m/s are present in 90 degree orientation and 75 degree orientation. Similar reductions are not present in the 60 degree arrangement.
- A jetting effect is not observed at the northeast entry gate, which is in contrast to the north oncoming wind.
- The high wind speeds present in the southwest corner were not significantly mitigated by any of the wind screen arrangements tested.
- The 75 degree wind screen orientation and 90 degree wind screen orientation reduce the pedestrian level wind speeds to near 3 m/s in much of the north half of the field and along the “back stretch”. There are some small regions where 4 m/s are present. The 60 degree wind screen orientation shows two regions in the northern area of the field where 4 m/s winds are more common.

SUMMARY OF RESULTS FOR WIND FROM THE NORTHWEST

- There are no dramatic improvements resulting from the wind screens when a northwest oncoming wind is active. Jetting effects are pronounced in the northwest corner at two locations resulting from the wind being diverted around and between buildings.
- The gap between the temporary seating and permanent seating at the southeast corner promotes the diagonal flow across the field with wind speeds of 7.5 m/s and greater.
- There are no observed relative advantages among the three wind screen orientations.

GRAPHIC RESULTS

Figures 3 through 14 illustrate the wind-tunnel results generated by Matlab v.7. Below each figure is a description of the results for its setting.

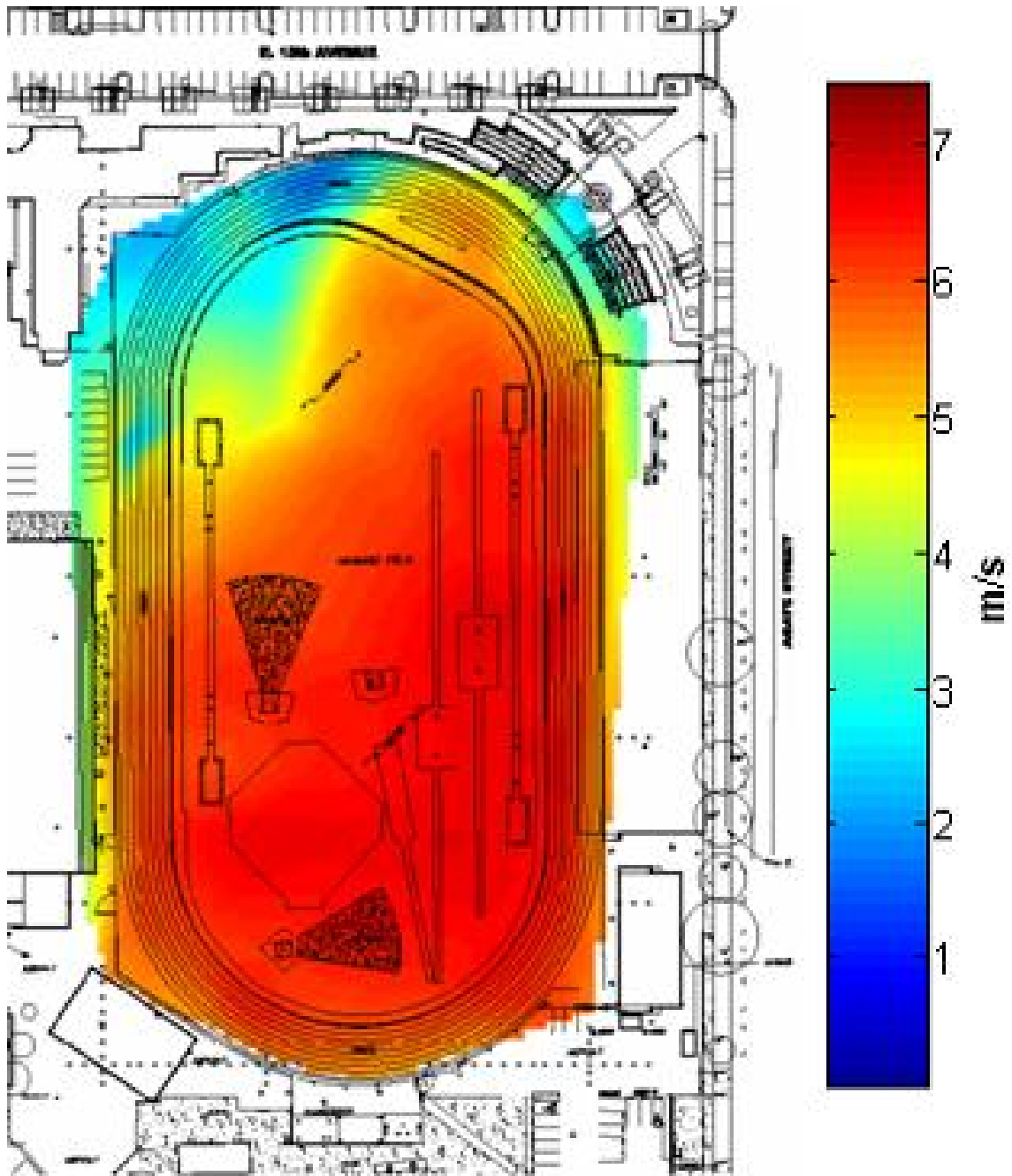


Figure 3. Predicted full-scale pedestrian level (5 feet or 1.5 meters above ground level) wind speeds are shown for a north oncoming wind without wind screen protection. The reference velocity is assumed to be 7.5 m/s at a reference height of 10 m. The results show that the field is dominated by wind speeds in excess of 6 m/s.

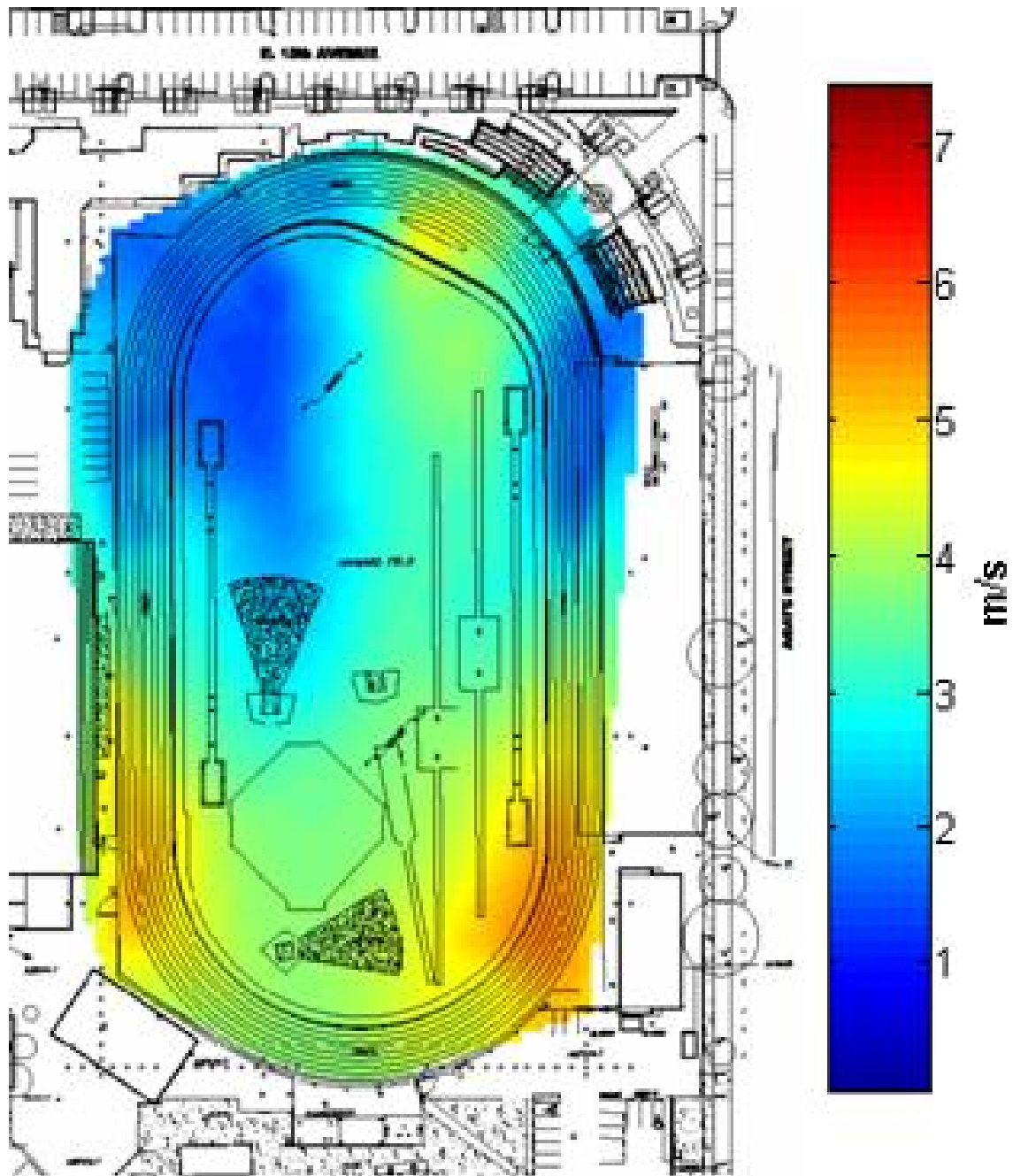


Figure 4. Predicted full-scale pedestrian level (5 feet or 1.5 meters above ground level) wind speeds are shown for a north oncoming wind with wind screen protection. All wind screens are positioned 90 degrees counter-clockwise from the north. The reference velocity is assumed to be 7.5 m/s at a reference height of 10 m. The results show reduction in the northwest corner below 2 m/s. There are three regions where the wind speed nearly reaches or exceeds 5 m/s.

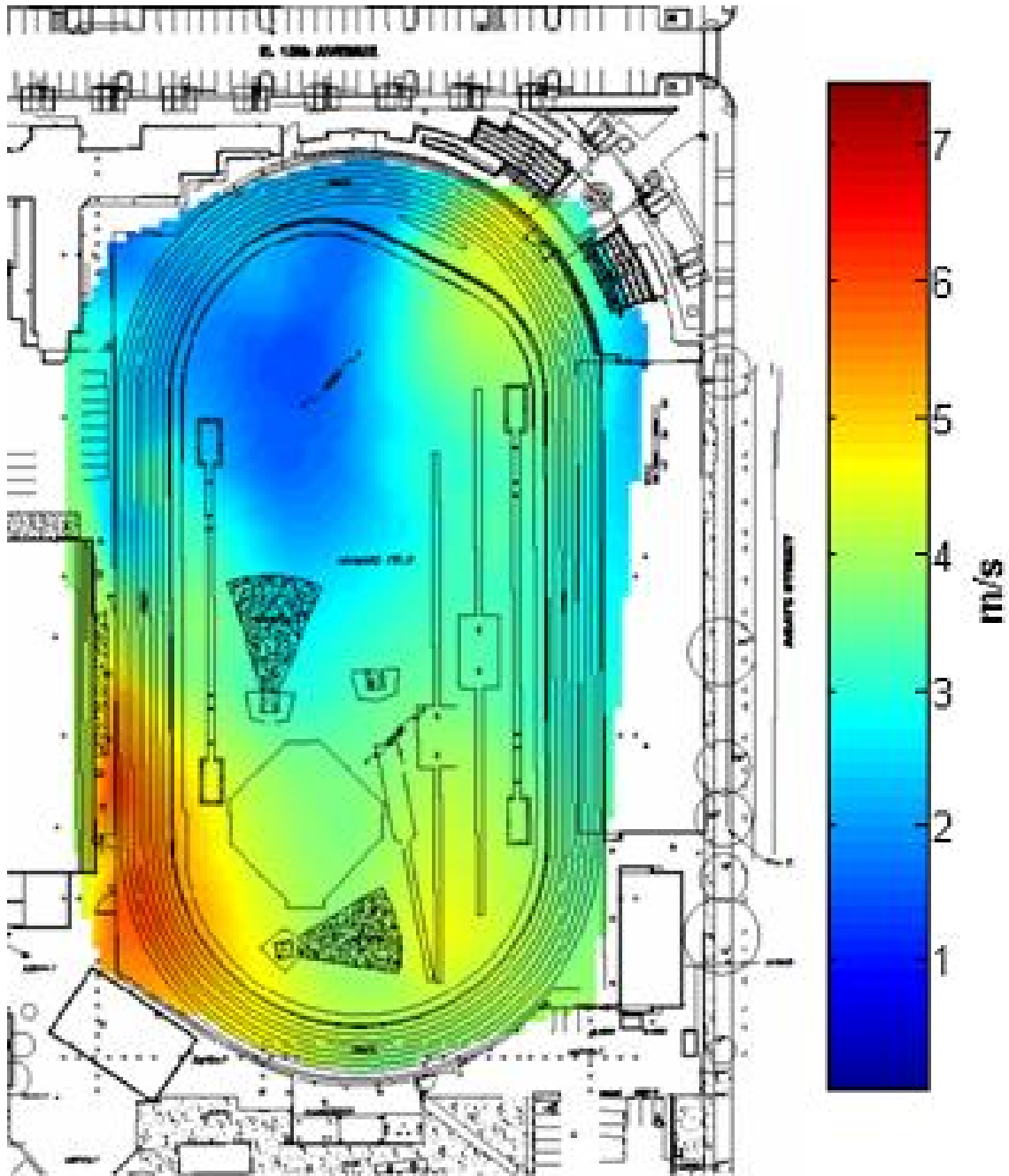


Figure 5. Predicted full-scale pedestrian level (5 feet or 1.5 meters above ground level) wind speeds are shown for a north oncoming wind with wind screen protection. All wind screens are positioned 75 degrees counter-clockwise from the north. The reference velocity is assumed to be 7.5 m/s at a reference height of 10 m. The results show reduction in the northwest corner below 2 m/s. Two regions show wind speeds of nearly 5 m/s and another shows speeds of 6 m/s. Relative to the 90 degree orientation, wind speed gains are prominent in the southwest corner.

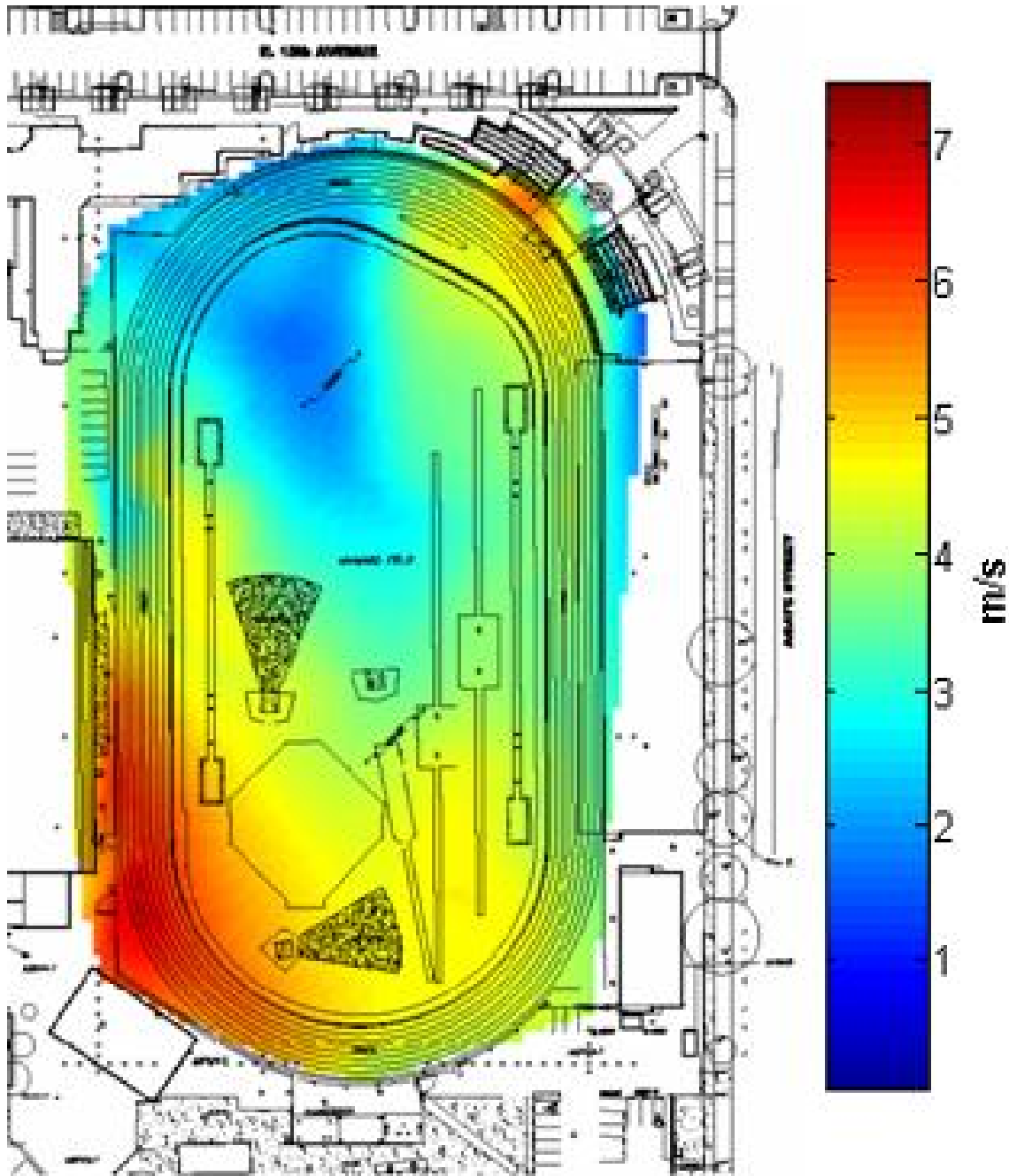


Figure 6. Predicted full scale pedestrian level (5 feet or 1.5 meters above ground level) wind speeds are shown for a north oncoming wind with wind screen protection. All wind screens are positioned 60 degrees counter-clockwise from the north. The reference velocity is assumed to be 7.5 m/s at a reference height of 10 m. The results show reduction in the northwest corner below 2 m/s. Relative to the 75 degree orientation, a jetting effects appear to increase through the entrance gate in the northeast corner and further wind speed gains appear in the southwest corner. Much of the field shows wind speeds between 4 m/s and 6 m/s.

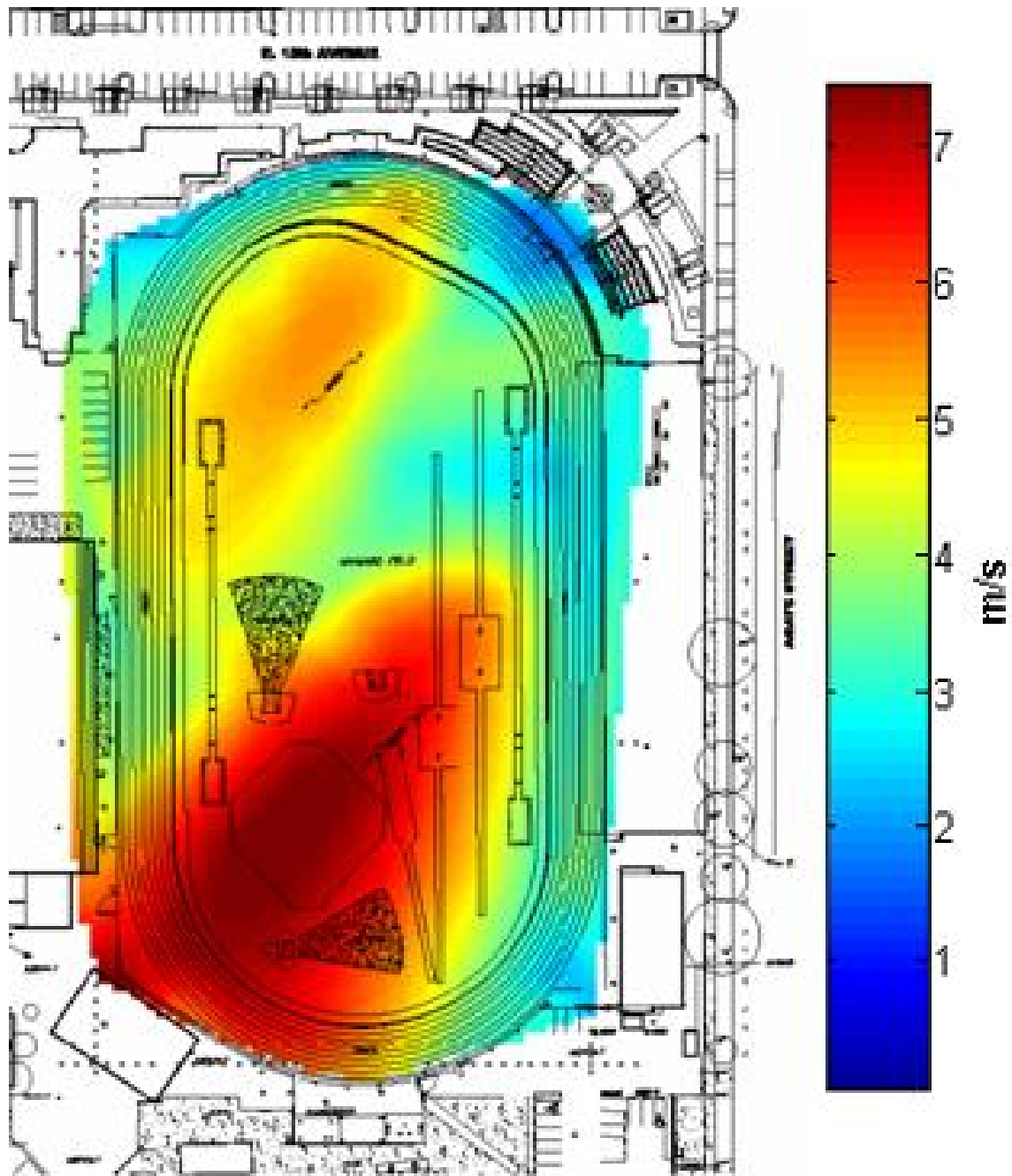


Figure 7. Predicted full-scale pedestrian-level (5 feet or 1.5 meters above ground level) wind speeds are shown for a northeast oncoming wind without wind screen protection. The reference velocity is assumed to be 7.5 m/s at a reference height of 10 m. The highest wind speeds exist in the southwest corner, which reach or exceed 7.5 m/s.

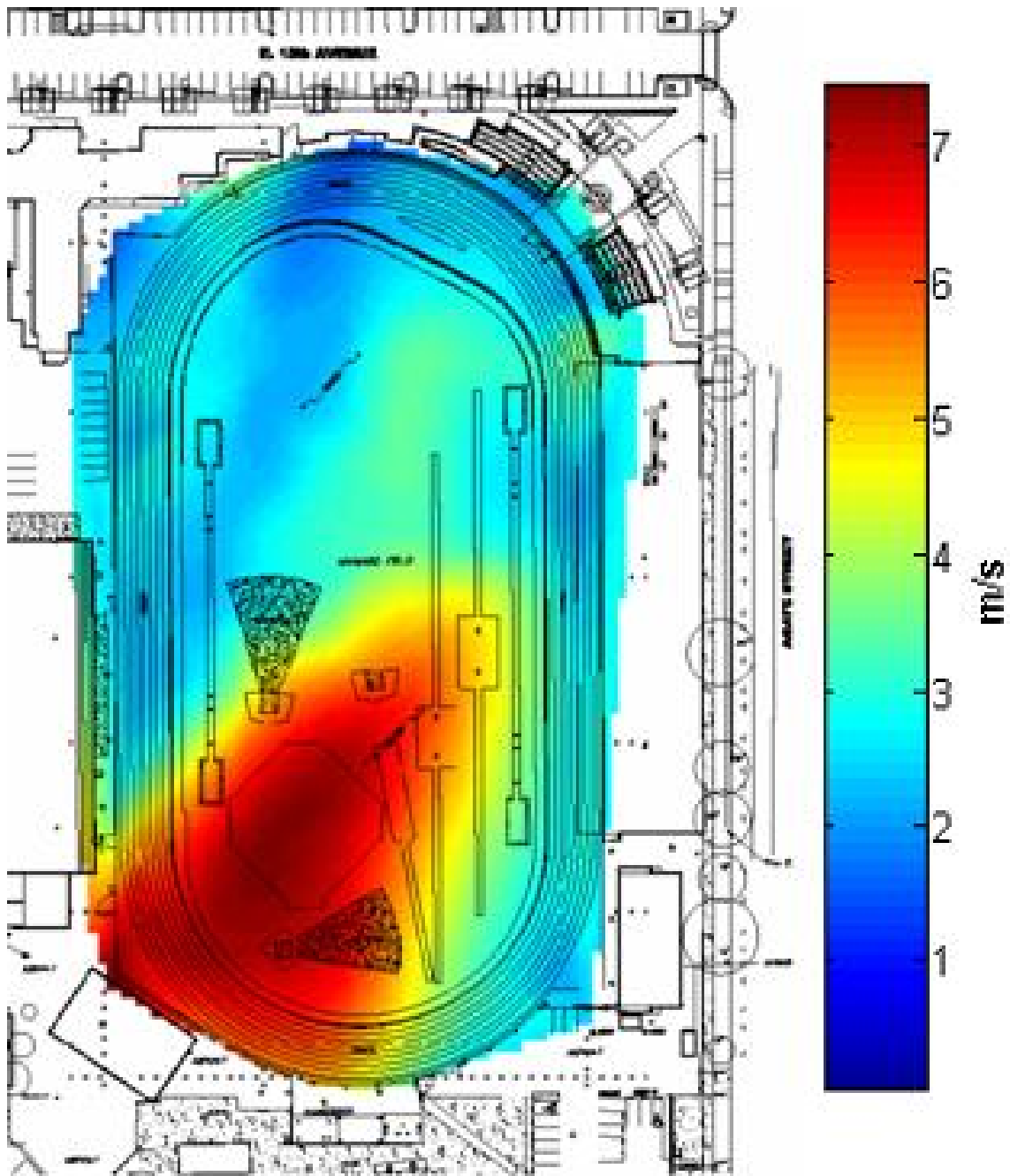


Figure 8. Predicted full-scale pedestrian level (5 feet or 1.5 meters above ground level) wind speeds are shown for a northeast oncoming wind with wind screen protection. All wind screens are positioned 90 degrees counter-clockwise from the north. The reference velocity is assumed to be 7.5 m/s at a reference height of 10 m. The results show few reductions in the northern region below 2 m/s. As was true for the existing case, wind speeds at or beyond 7.5 m/s are present in the southwest corner. Wind speeds at or near 3 m/s are prevalent over much of the field.

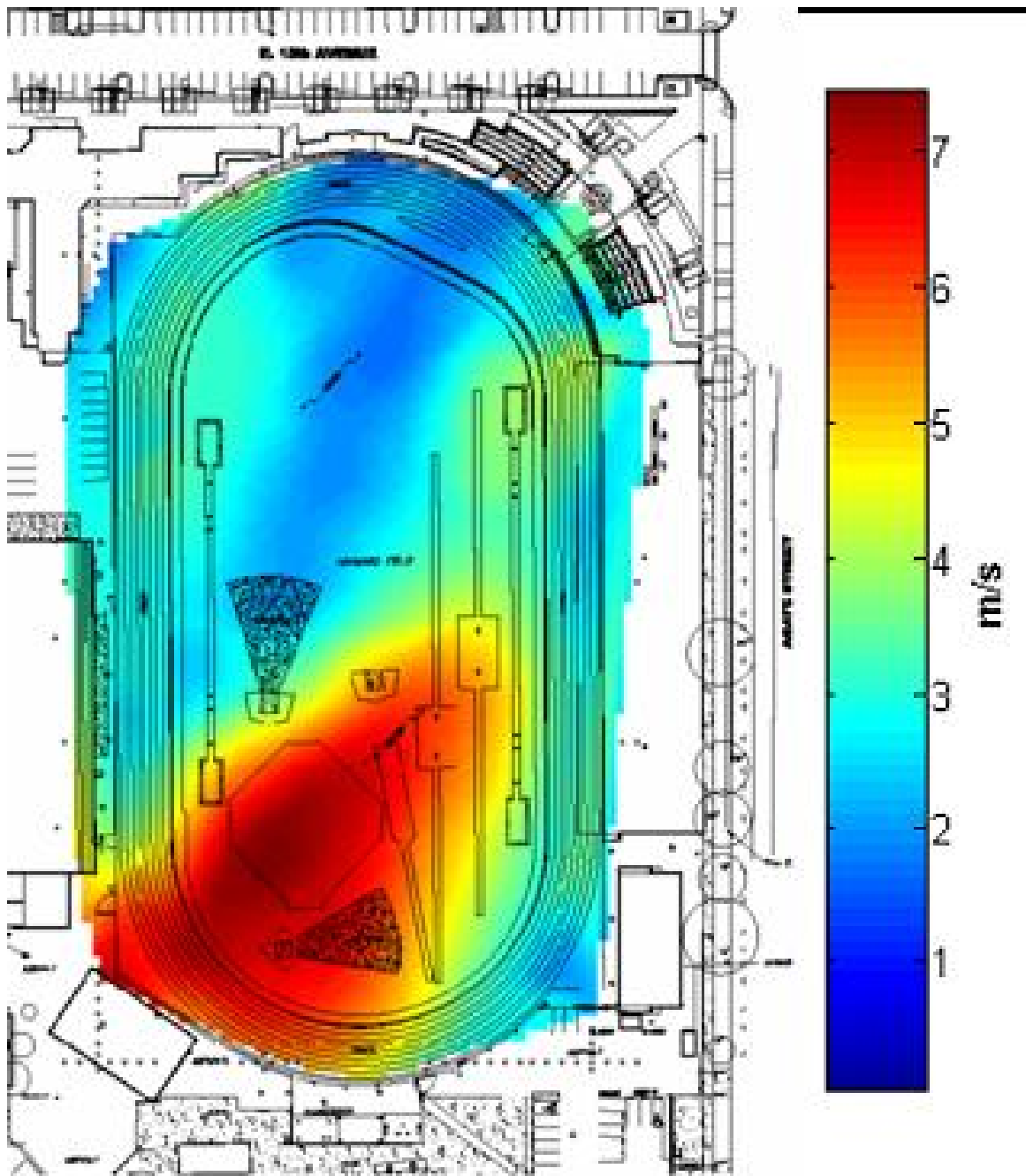


Figure 9. Predicted full-scale pedestrian level (5 feet or 1.5 meters above ground level) wind speeds are shown for a northeast oncoming wind with wind screen protection. All wind screens are positioned 75 degrees counter-clockwise from the north. The reference velocity is assumed to be 7.5 m/s at a reference height of 10 m. The results show some reductions in the northern region below 2 m/s. As was true for the existing case, wind speeds at or beyond 7.5 m/s are present in the southwest corner. Wind speeds near 3 m/s are prevalent over much of the field.

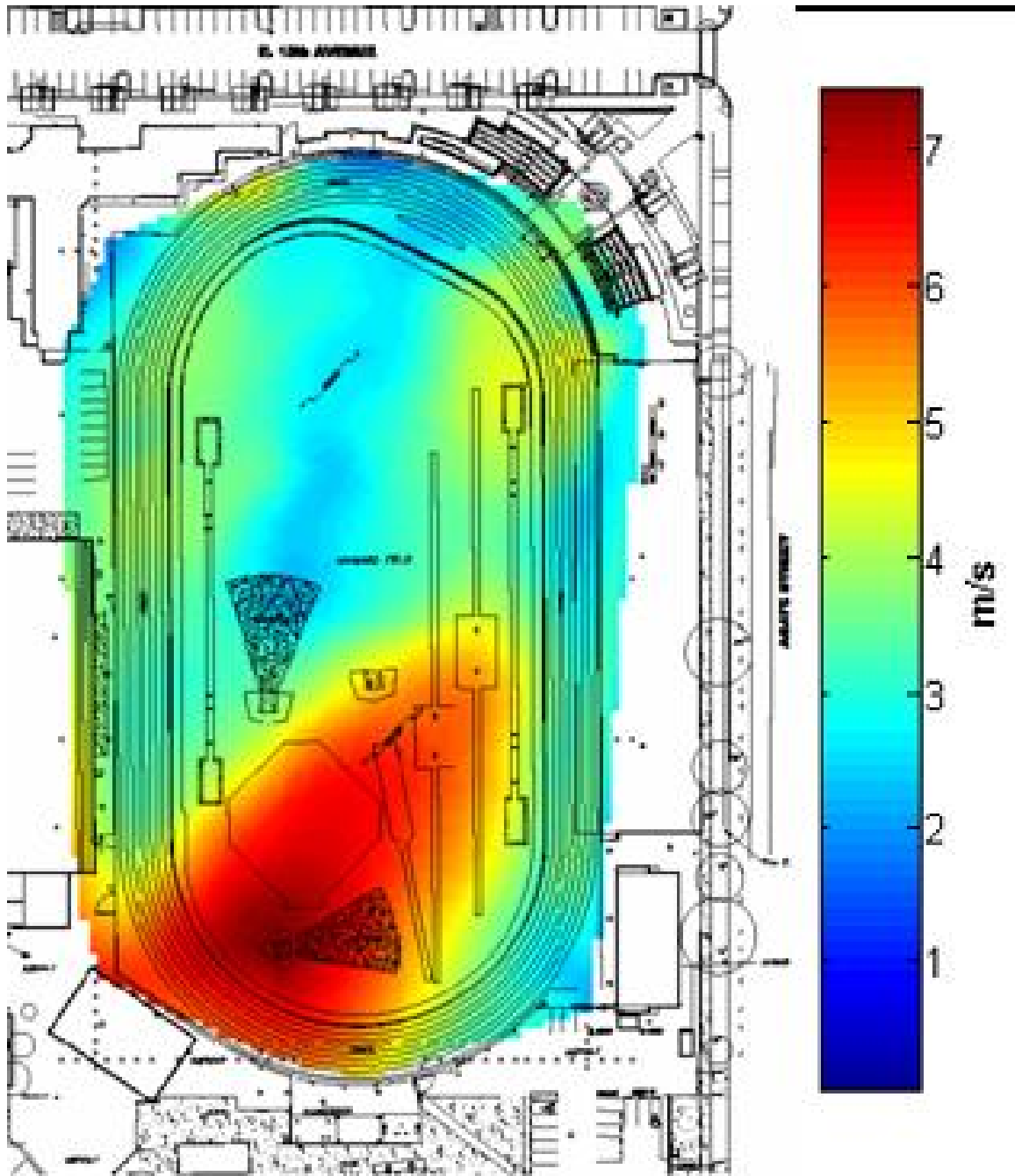


Figure 10. Predicted full-scale pedestrian level (5 feet or 1.5 meters above ground level) wind speeds are shown for a northeast oncoming wind with wind screen protection. All wind screens are positioned 60 degrees counter-clockwise from the north. The reference velocity is assumed to be 7.5 m/s at a reference height of 10 m. Fewer reductions are present in the northern region relative to the 90 degree and 75 degree orientations. As was true for the existing case, wind speeds at or beyond 7.5 m/s are present in the southwest corner. Wind speeds between 3 m/s and 4 m/s are prevalent over much of the field.

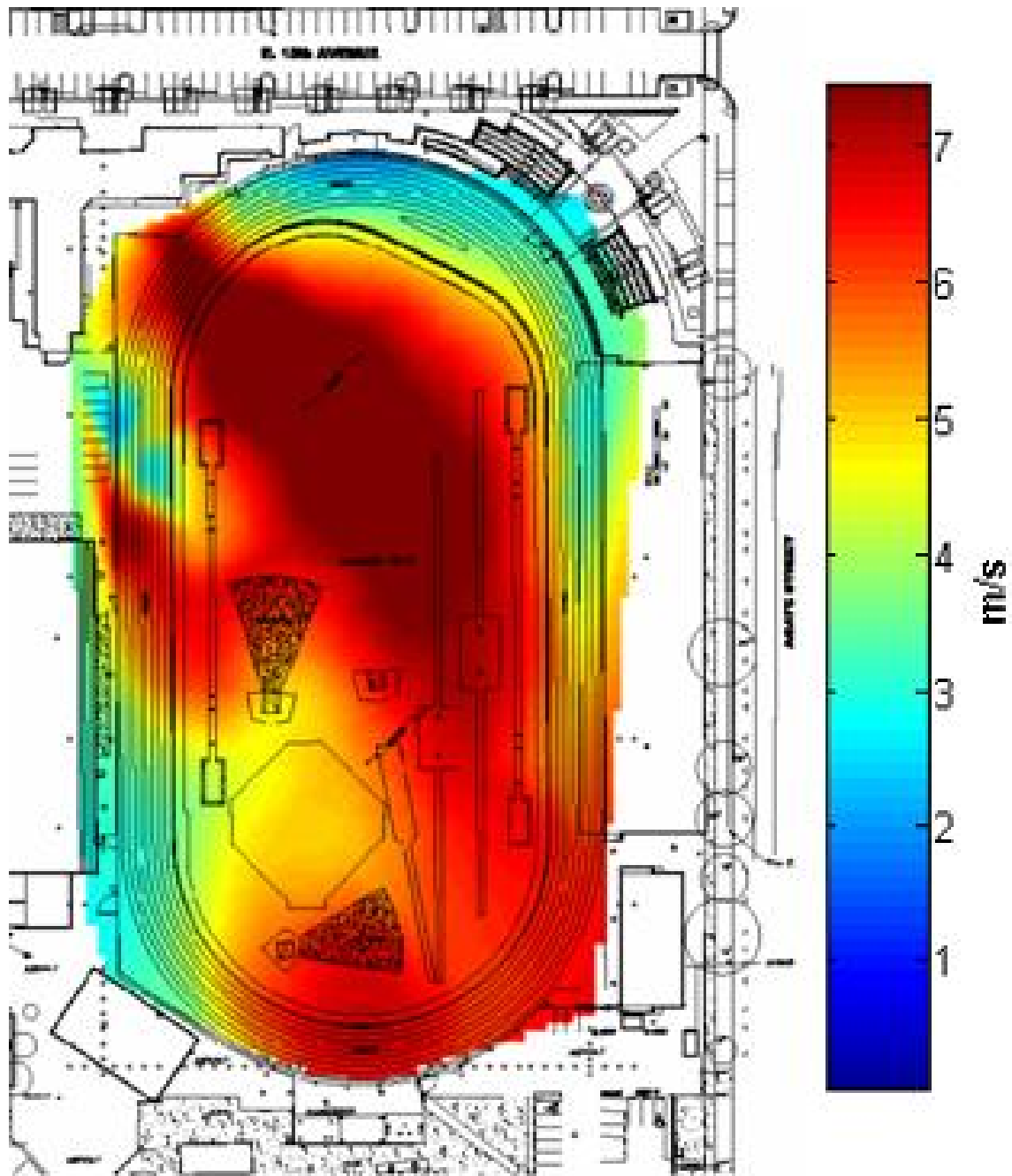


Figure 11. Predicted full-scale pedestrian level (5 feet or 1.5 meters above ground level) wind speeds are shown for a northwest oncoming wind without wind screen protection. The reference velocity is assumed to be 7.5 m/s at a reference height of 10 m. The highest wind speeds, which reach or exceed 7.5 m/s, exist in the northern region of the field.

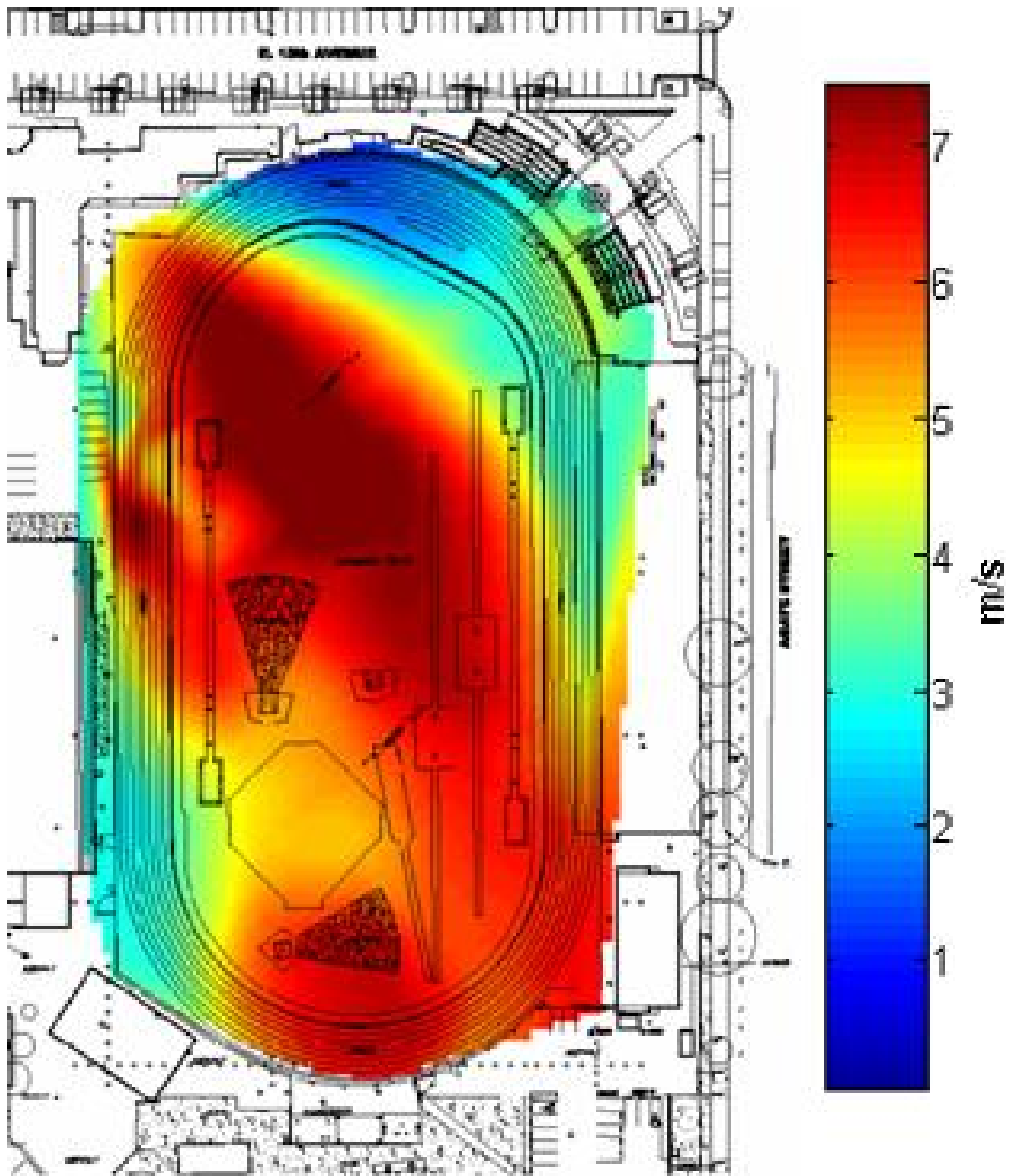


Figure 12. Predicted full-scale pedestrian level (5 feet or 1.5 meters above ground level) wind speeds are shown for a northwest oncoming wind with wind screen protection. All wind screens are positioned 90 degrees counter-clockwise from the north. The reference velocity is assumed to be 7.5 m/s at a reference height of 10 m. The results show few reductions in the northern region below 2 m/s. As was true for the existing case, wind speeds at or beyond 7.5 m/s are present in the northern region.

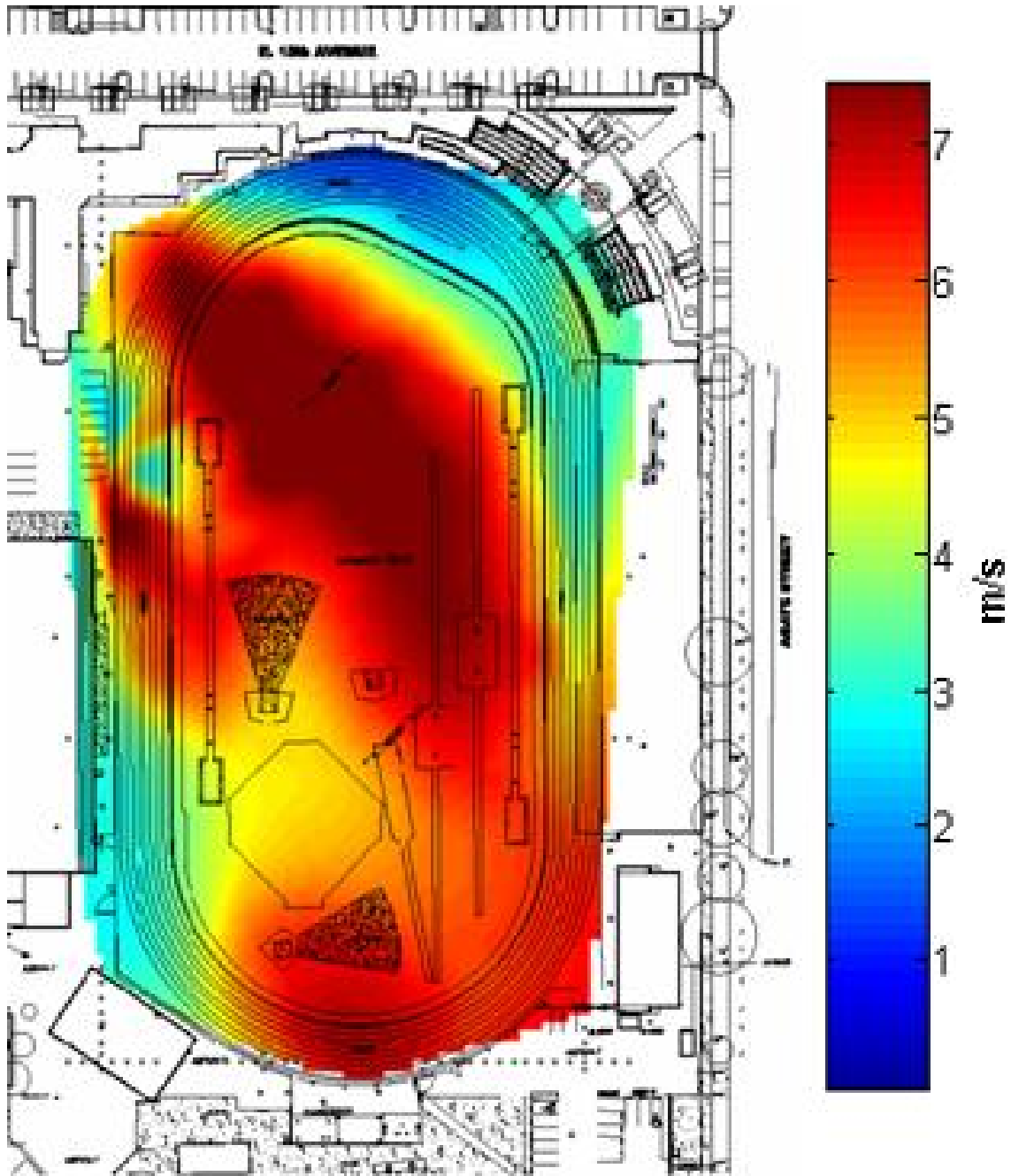


Figure 13. Predicted full-scale pedestrian level (5 feet or 1.5 meters above ground level) wind speeds are shown for a northwest oncoming wind with wind screen protection. All wind screens are positioned 75 degrees counter-clockwise from the north. The reference velocity is assumed to be 7.5 m/s at a reference height of 10 m. The results show few reductions in the northern region below 2 m/s. As was true for the existing case, wind speeds at or beyond 7.5 m/s are present in the northern region.

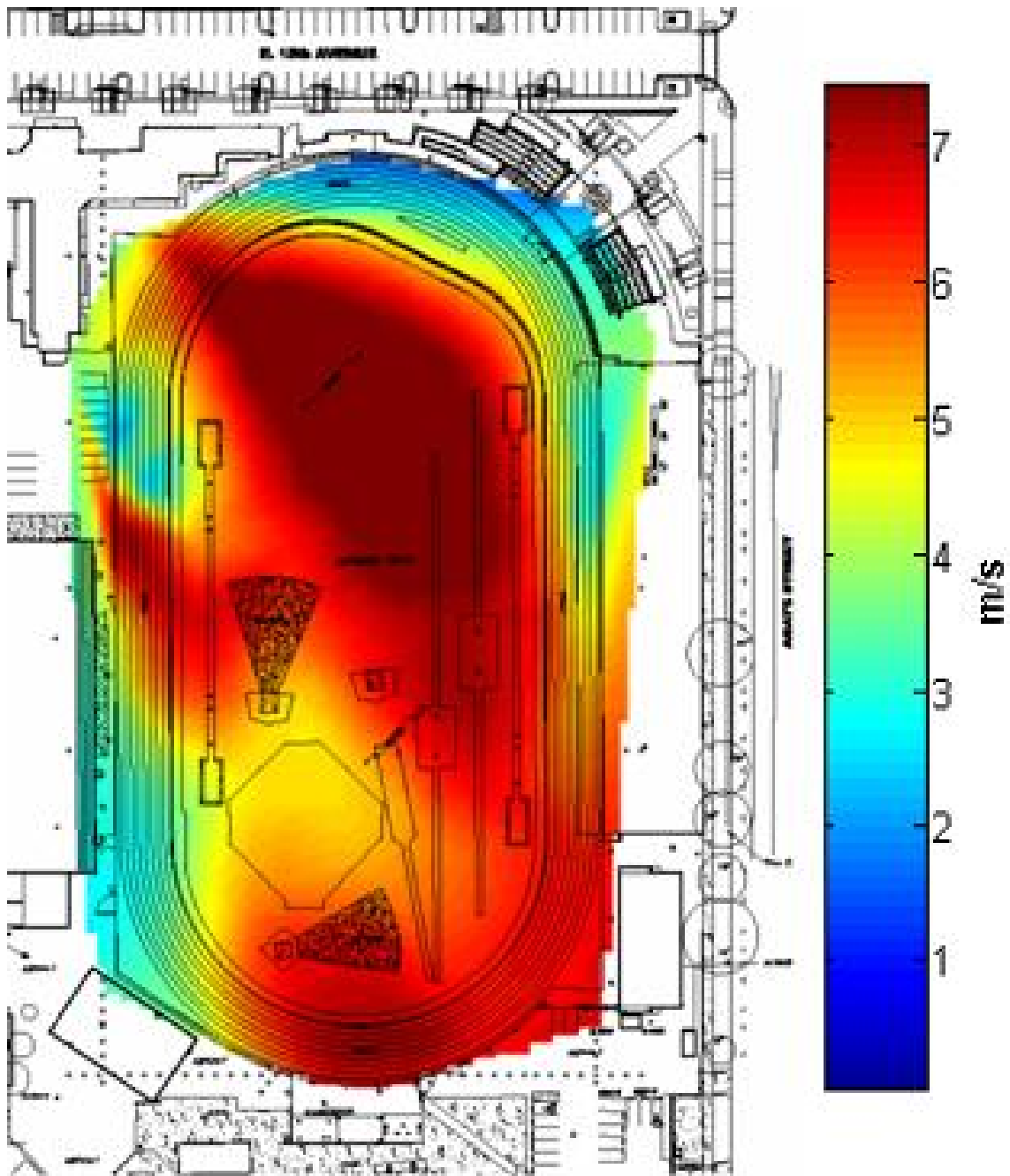


Figure 14. Predicted full-scale pedestrian level (5 feet or 1.5 meters above ground level) wind speeds are shown for a northwest oncoming wind with wind screen protection. All wind screens are positioned 60 degrees counter-clockwise from the north. The reference velocity is assumed to be 7.5 m/s at a reference height of 10 m. The results show few reductions in the northern region below 2 m/s. As was true for the existing case, wind speeds at or beyond 7.5 m/s are present in the northern region.

WIND-TUNNEL PROFILE RESULTS

Velocity profiles were taken at 10 points on the field at heights of 40, 50 and 60 feet (12.2, 15.2 and 18.3 meters), full scale, for the existing and 90 degree settings with winds from the north. The progress of points is from a north to south orientation as presented in Table 1; and, they are illustrated in Figure 2 as measurement locations with black outlining circles around the numbered location. Results are in meters per second assuming a wind speed of 7.5 meters per second at a height of 10 meters above ground-level and are displayed in Table 1 below.

Table 1. Velocity profiles taken in the wind tunnel at equivalent heights of 40, 50 and 60 feet (12.2, 15.2 and 18.3 meters) above ground, full scale. Estimated full-scale velocities are shown in meters per second and assume a north wind of 7.5 meters per second at a height of 10 meters above the ground.

<i>Existing - no screens</i>				<i>Screens 90 degrees to the wind</i>			
heights	40 ft	50 ft	60 ft	heights	40 ft	50 ft	60 ft
#	[12.2 m]	[15.2 m]	[18.3 m]	#	[12.2 m]	[15.2 m]	[18.3 m]
35	8.5973	9.4286	9.3636	35	3.8964	4.5492	6.1022
45	8.5731	8.9135	9.4796	45	3.9449	4.6958	6.2118
54	8.5310	9.0270	9.5536	54	4.0226	5.0567	6.4337
61	8.5234	8.8562	9.3164	61	4.5135	5.5042	6.9577
67	8.5476	8.9480	9.4159	67	4.3452	5.3078	6.3023
76	8.5833	9.1494	9.4694	76	4.7558	5.8790	6.8812
84	8.5451	8.8982	9.4567	84	5.1752	5.9823	7.3121
92	8.4074	9.1392	9.0971	92	6.0269	7.0673	7.5518
97	8.2748	8.6764	9.1507	97	6.4337	7.3172	7.9662
106	8.4762	8.7312	8.9378	106	6.4171	7.1464	7.8145

PEDESTRIAN RESULTS

Receptor locations not located on the field are referred to in this text as pedestrian points. Pedestrian points are measurement locations #1 through #16, #119, #121 and #122. Table 2 describes their approximate locations relative to various structures on the site. Table 3 gives the estimated equivalent full-scale velocities encountered at a height of 5 feet (1.5 meters) above the ground in meters per second, assuming a wind speed of 7.5 meters per second at a height of 10 meters above the ground.

Table 2. Locations of pedestrian points #1-16, #119, #121 and #122.

#	Point Location Description
1	Between Screens 3 and 4
2	Between Screens 4 and 5; trees lie to the south
3	Between Screens 5 and 6; trees lie to the south
4	Between Screens 6 and 7; trees lie to the southwest
5	Between Screens 7 and 8
6	East of Screen 6 and north of Screen 9
7	The most northern pedestrian point; north of Point 8 and northwest of Point 9; not directly near a screen
8	Directly south of Point 7, and directly west of Point 9; not directly near a screen
9	Directly east of Point 8; most northeastern point; not directly near a screen
10	Between Screens 9 and 10; point nearest to the entrance
11	Directly north of Screen 10; east of Point 10
12	Between Screens 10 and 11; in the middle of three small trees
13	Directly south of Point 9, by a large tree; south-southeast of Screen 11
14	Directly south of Points 9 and 13
15	Directly south of Points 9, 13, and 14; surrounded by trees to the north and south
16	Directly south of points 9, 13, 14, and 15; several trees lie to the north and a small tree to the south
119	Between Screens 2 and 3
121	Between Screens 1 and 2
122	The most western point. West of Screen 1

***Notes**

Points are centered between the actual opening between the screens (when oriented east-west).

Table 3. Equivalent estimated full-scale velocities, in meters per second, at each pedestrian point at an equivalent height of 5 feet (1.5 meters) above the ground for a wind speed of 7.5 meters per second at a height of 10 meters above the ground, organized by screen orientation and wind direction.

Existing				90 degrees to the wind				75 degrees to the wind				60 degrees to the wind			
#	N	NW	NE	#	N	NW	NE	#	N	NW	NE	#	N	NW	NE
1	3.1378	4.3592	2.6558	1	4.8221	6.1073	4.6346	1	4.3758	6.9564	3.6567	1	3.8696	7.4728	3.3749
2	3.5942	4.4931	2.6711	2	5.7337	5.9683	5.4022	2	5.0222	6.6045	4.9062	2	4.7188	6.9743	4.1591
3	3.2857	4.4204	2.4429	3	5.3308	5.8969	5.7248	3	4.3554	6.2921	5.5743	3	4.2292	6.4515	4.8909
4	4.1042	4.5518	3.5942	4	4.8055	6.3023	6.2883	4	4.2075	6.6338	6.2093	4	4.2713	6.3215	5.7477
5	3.0855	3.9908	4.3516	5	4.4523	6.4630	7.3440	5	4.3312	6.4273	6.9743	5	4.5365	6.1544	6.9755
6	5.6980	3.6121	5.8752	6	4.5110	5.8931	5.2288	6	4.3325	6.5242	5.0732	6	4.3388	5.9109	5.6113
7	3.3953	4.6627	6.6632	7	5.0108	5.4111	6.5267	7	4.1782	5.7197	6.3967	7	4.1055	5.6355	6.8506
8	3.6325	4.8068	4.9343	8	5.5858	5.4226	4.9253	8	4.7303	5.5514	4.5441	8	4.7927	5.8523	4.7685
9	3.0383	4.9432	5.1357	9	4.5390	5.5399	4.3325	9	3.8747	5.8191	4.8616	9	3.7485	5.6929	5.1803
10	6.0843	4.1438	5.8829	10	6.2309	4.5224	5.2556	10	5.5781	4.6627	4.9355	10	5.6738	4.6168	5.1268
11	5.5463	4.6385	4.8935	11	6.0410	4.8246	4.9534	11	5.5565	5.0860	4.5454	11	5.5106	5.0503	4.7621
12	4.9202	4.3567	4.3159	12	8.0249	4.5926	5.1523	12	7.3670	4.5008	4.7315	12	7.0304	4.4855	4.6958
13	3.5764	5.1395	2.9096	13	3.8594	4.6244	2.3855	13	4.1948	3.9219	2.5054	13	4.8412	3.4731	2.6954
14	2.4697	2.4378	2.5921	14	2.4722	1.7901	2.6150	14	2.5411	1.8207	2.5717	14	3.1340	1.8704	2.4034
15	3.5024	1.5644	3.9908	15	3.2347	1.3630	3.9614	15	3.2831	1.3872	3.9066	15	3.2436	1.3847	3.8798
16	2.8101	5.4723	6.2985	16	2.3039	5.7362	6.3737	16	2.6125	5.6738	6.1583	16	2.9236	5.5934	6.1085
119	3.6503	4.5263	3.7664	119	4.7532	5.5820	5.1803	119	4.2254	7.0482	4.0698	119	4.1680	7.6985	3.5254
121	3.4374	4.6436		121	5.2849	6.0448		121	5.2466	6.3329		121	4.5734	7.4116	
122	2.7209	4.5403		122	4.9062	3.3456		122	5.2951	3.5381		122	5.6036	3.9933	

points were out of bounds for wind-tunnel measurements

6. MITIGATION SUGGESTIONS

To further reduce the wind speeds at pedestrian level on the Hayward field a number of mitigation measures may be taken. A summarize of these suggestions for mitigation of non-performing areas are: i) Creating a solid non-porous gate-entrance area at the northeast corner of Hayward Field should improve the “jetting” effect both at the entrance area and on the northeast corner of Hayward Field itself, including the running track area; ii) Increase the physical height and/or horizontal spacing between pylon screens to extend the wind shelter area downwind of the screens, i.e., increase the recovery distance of the air speed over the middle to south end of the field; iii) Extend the south bleachers to completely enclose the south end of the track. This would in principle stop the surface level wind, thus forcing the wind to pass over the bleachers which in turn may shelter the south-end area including the running track. This might also reduce or substantially decrease the two “jetting” areas that are observed in Figures 4 as the orange to red areas on the southwest and southeast areas of the running track. This effect might also be achieved by constructing solid-walls and/or barriers across the south end of Hayward field; these must be a continuous blockage of surface level wind from the western seating stands to the eastern stadium seating stands.

7. CONCLUDING REMARKS

The present wind-tunnel investigation was performed in the Atmospheric Boundary Layer Wind Tunnel (ABLWT) located at University of California, Davis (UCD). The study was independent of the University. A detailed description of the facility is given in Appendix A. Testing was conducted using a one inch on the model equals 20 feet full scale) scaled-model centered on Hayward Field.

A wind-tunnel study of the pedestrian-level wind environment was conducted for the proposed Hayward Field renovation project. Tests were conducted for three wind directions: north, northeast and northwest. Results were analyzed using a given reference wind speed of 16.8 miles per hour (7.5 meters per second) at a height of 32.8 feet (10 meters) above ground level.

The main objective of the test was to predict the wind speeds that would exist on the site for the determination of the various pylons' wind screen orientations. One hundred twenty-two surface points were measured to evaluate the site and estimate corresponding full-scale wind speeds.

8. REFERENCES

- Arens, E. 1981 “Designing for an acceptable wind environment”, *Trans. Engrg., ASCE*, Vol. 107, No. Te 2, pp 127-141.
- Arens, E., C., D. Ballanti, C.B. Bennett, S. Guldman, and B.R. White 1989 “Developing the San Francisco wind ordinance and its guidelines for compliance”, *Building and Environment*, Vol. 24, No. 4, pp 297-303.
- Davenport, A.G. 1961 “The application of statistical concept of wind loading of structures”, *Proc. Inst. Civil Engrg.*, 19, 449-472.
- Hunt, J.C.R., E.C. Poulton, and J.C. Mumford 1976 “The effects of wind on people: new criteria based on wind tunnel experiments,” *Building and Environment*, Vol. 13, pp 251-260.
- Jackson, P.S. 1978 “The evaluation on windy environments,” *Building and Environment* 13, pp 251-260.
- Kuspa, B. K. 2006. *Urban Wind Power Assessment: A Study of Winds over the Near Surfaces of Several Buildings in San Francisco*. Unpublished Master of Science thesis, University of California, Davis, Davis, California, United States of America.
- Melbourne, W.H. 1978 “Criteria for environmental wind conditions,” *Journal Wind Engineering and Industrial Aerodynamics* , Vol. 3, pp 241-249.
- Penwarden, A.D. 1973 “Acceptable wind speeds in towers,” *Building Science*, Vol. 8 No. 3, pp 259-267.
- White, B. R. 1991 “Analysis and wind-tunnel simulation of pedestrian-level winds in San Francisco, *Journal Wind Engineering and Industrial Aerodynamics*, Vol. 41, pp 2353-2364.
- White, B. R. 1991 “Analysis and wind-tunnel simulation of pedestrian-level winds in San Francisco, *Proceedings of the Eight International Conference on Win Engineering*, University of Western Ontario, London, Ontario, Canada, July 8-12.
- White, B. R. 1994 “Wind-tunnel simulation of pedestrian level wind in Los Angeles,” *Proceedings of the 2nd United Kingdom Wind Engineering Conference*, Wind Engineering Society, held at University of Warwick, England, September 19-22.

APPENDIX A. WIND-TUNNEL RESULTS

The wind-tunnel results are provided in following pages and include the coordinates of the measurement locations (full scale, in tabular form), the estimated full-scale wind speeds, the turbulent intensity values (in percentages) observed in the wind tunnel and the R-values obtained during the wind-tunnel test. For the estimated full-scale wind speed table, all wind speeds in excess of 2 meters per second are highlighted in yellow, and speeds below 1.5 meters per second are highlighted in green. The turbulent intensity table illustrates all values exceeding 50 percent in red text, and the R-values table displays all R-values above 0.5 in red text.

Hayward Field 1-07

Scale: 1" WT = 20' FS

Full Scale in Feet

*origin of axis is at the southwestern corner of the model

*E is x axis

*N is y axis

	x _{FS} [ft]	y _{FS} [ft]		x _{FS} [ft]	y _{FS} [ft]		x _{FS} [ft]	y _{FS} [ft]		x _{FS} [ft]	y _{FS} [ft]		x _{FS} [ft]	y _{FS} [ft]		x _{FS} [ft]	y _{FS} [ft]		x _{FS} [ft]	y _{FS} [ft]		x _{FS} [ft]	y _{FS} [ft]		
1.	176.38	709.45	26.	185.04	614.96	51.	129.13	518.90	76.	219.69	375.59	101.	113.39	196.06											
2.	221.26	708.66	27.	211.81	604.72	52.	162.99	503.15	77.	283.46	377.17	102.	99.21	148.03											
3.	266.14	709.45	28.	257.48	604.72	53.	201.57	501.57	78.	334.65	378.74	103.	129.13	157.48											
4.	309.45	709.45	29.	300.79	603.94	54.	244.09	501.57	79.	373.23	380.31	104.	151.18	172.44											
5.	367.48	709.45	30.	330.71	614.17	55.	286.61	499.21	80.	395.28	381.10	105.	200.00	170.87											
6.	403.94	710.24	31.	383.46	598.43	56.	335.43	499.21	81.	106.30	320.47	106.	251.97	170.08											
7.	469.29	711.02	32.	149.61	574.80	57.	395.28	492.91	82.	129.92	336.22	107.	307.09	170.08											
8.	468.50	690.55	33.	173.23	570.87	58.	125.98	462.20	83.	161.42	331.50	108.	362.20	181.89											
9.	489.76	687.40	34.	203.94	571.65	59.	165.35	463.78	84.	217.32	328.35	109.	155.12	126.77											
10.	430.71	670.87	35.	240.94	567.72	60.	201.57	464.57	85.	283.94	327.56	110.	188.98	135.43											
11.	446.46	669.29	36.	284.25	566.93	61.	244.09	465.35	86.	334.65	324.41	111.	334.65	144.88											
12.	462.99	622.05	37.	335.43	572.44	62.	286.04	466.14	87.	375.59	348.03	112.	381.89	158.27											
13.	492.13	544.88	38.	373.23	569.06	63.	333.86	462.20	88.	390.55	318.11	113.	210.24	96.85											
14.	489.76	451.18	39.	393.70	568.50	64.	376.38	466.14	89.	107.09	270.08	114.	239.37	115.75											
15.	490.55	314.17	40.	437.01	551.97	65.	108.66	432.28	90.	127.56	296.85	115.	268.50	86.61											
16.	488.98	134.65	41.	75.59	535.43	66.	159.84	419.69	91.	180.31	281.10	116.	296.85	121.26											
17.	259.06	663.78	42.	116.54	477.95	67.	216.54	425.20	92.	249.61	284.25	117.	320.47	102.36											
18.	325.20	648.82	43.	162.99	537.01	68.	279.53	425.20	93.	322.83	281.89	118.	407.09	129.92											
19.	396.85	631.50	44.	203.15	535.43	69.	333.86	425.20	94.	381.10	287.40	119.	133.07	708.66											
20.	188.19	643.31	45.	241.73	534.65	70.	376.38	414.17	95.	129.13	241.73	120.	85.83	196.06											
21.	233.86	633.07	46.	288.19	531.50	71.	396.06	441.73	96.	186.61	233.07	121.	87.40	708.66											
22.	288.98	633.07	47.	336.22	529.13	72.	129.92	399.21	97.	251.18	229.13	122.	33.07	707.87											
23.	362.20	624.41	48.	374.80	522.05	73.	104.72	371.65	98.	315.75	232.28														
24.	105.51	607.87	49.	398.43	537.80	74.	134.65	377.17	99.	377.17	242.52														
25.	141.73	607.09	50.	106.30	486.61	75.	162.99	377.17	100.	396.85	226.77														

Hayward Field 2-2-07 - Uped_{FS} Values [m/s] conversion 1.7 Uref_{FS} = 7.5 m/s

Existing				90 degrees to the wind				75 degrees to the wind				60 degrees to the wind			
#	N	NW	NE	#	N	NW	NE	#	N	NW	NE	#	N	NW	NE
1	3.1378	4.3592	2.6558	1	4.8221	6.1073	4.6346	1	4.3758	6.9564	3.6567	1	3.8696	7.4728	3.3749
2	3.5942	4.4931	2.6711	2	5.7337	5.9683	5.4022	2	5.0222	6.6045	4.9062	2	4.7188	6.9743	4.1591
3	3.2857	4.4204	2.4429	3	5.3308	5.8969	5.7248	3	4.3554	6.2921	5.5743	3	4.2292	6.4515	4.8909
4	4.1042	4.5518	3.5942	4	4.8055	6.3023	6.2883	4	4.2075	6.6338	6.2093	4	4.2713	6.3215	5.7477
5	3.0855	3.9908	4.3516	5	4.4523	6.4630	7.3440	5	4.3312	6.4273	6.9743	5	4.5365	6.1544	6.9755
6	5.6980	3.6121	5.8752	6	4.5110	5.8931	5.2288	6	4.3325	6.5242	5.0732	6	4.3388	5.9109	5.6113
7	3.3953	4.6627	6.6632	7	5.0108	5.4111	6.5267	7	4.1782	5.7197	6.3967	7	4.1055	5.6355	6.8506
8	3.6325	4.8068	4.9343	8	5.5858	5.4226	4.9253	8	4.7303	5.5514	4.5441	8	4.7927	5.8523	4.7685
9	3.0383	4.9432	5.1357	9	4.5390	5.5399	4.3325	9	3.8747	5.8191	4.8616	9	3.7485	5.6929	5.1803
10	6.0843	4.1438	5.8829	10	6.2309	4.5224	5.2556	10	5.5781	4.6627	4.9355	10	5.6738	4.6168	5.1268
11	5.5463	4.6385	4.8935	11	6.0410	4.8246	4.9534	11	5.5565	5.0860	4.5454	11	5.5106	5.0503	4.7621
12	4.9202	4.3567	4.3159	12	8.0249	4.5926	5.1523	12	7.3670	4.5008	4.7315	12	7.0304	4.4855	4.6958
13	3.5764	5.1395	2.9096	13	3.8594	4.6244	2.3855	13	4.1948	3.9219	2.5054	13	4.8412	3.4731	2.6954
14	2.4697	2.4378	2.5921	14	2.4722	1.7901	2.6150	14	2.5411	1.8207	2.5717	14	3.1340	1.8704	2.4034
15	3.5024	1.5644	3.9908	15	3.2347	1.3630	3.9614	15	3.2831	1.3872	3.9066	15	3.2436	1.3847	3.8798
16	2.8101	5.4723	6.2985	16	2.3039	5.7362	6.3737	16	2.6125	5.6738	6.1583	16	2.9236	5.5934	6.1085
17	2.1586	1.7098	1.9189	17	2.8790	1.2355	1.4408	17	2.0783	1.2865	1.5899	17	2.1943	1.4204	1.6052
18	4.1756	2.6495	3.0689	18	3.3979	2.2083	2.3358	18	3.2168	1.9010	1.9967	18	3.6236	1.6537	2.4735
19	2.1152	2.5373	3.1378	19	3.0320	2.8994	3.5152	19	2.7693	2.8930	3.5828	19	2.4926	2.0528	3.4935
20	2.6010	2.7400	2.3549	20	2.5054	1.4357	3.8084	20	2.2351	1.9380	3.9538	20	1.9061	2.4926	4.6614
21	1.8845	2.7935	3.7026	21	2.1369	1.4331	1.5593	21	2.1152	1.9355	1.9508	21	2.2797	2.8930	3.0536
22	4.6627	2.7221	4.8017	22	3.4731	1.8398	2.5003	22	2.3843	1.5976	2.3690	22	3.5394	2.6954	2.6138
23	4.0711	2.8203	1.8462	23	3.1174	3.2028	2.1089	23	4.4778	2.8853	2.0668	23	5.6432	2.1076	3.2704
24	2.2351	3.8620	2.3575	24	1.6677	4.3924	1.5300	24	1.6652	4.4383	1.5708	24	2.0489	3.3188	1.7378
25	2.2313	7.1872	2.5041	25	1.8105	4.8705	2.4569	25	2.1675	5.9976	2.8318	25	2.4837	6.1213	2.9950
26	3.3112	4.1042	3.3928	26	1.9610	2.7999	2.9746	26	2.3345	3.7587	3.0970	26	2.4212	5.0936	3.5585
27	2.5883	4.7468	4.3108	27	2.2160	3.0269	1.8653	27	2.0783	4.5849	2.1446	27	2.4327	5.9109	2.8713
28	4.7685	4.5569	4.9853	28	2.5487	1.9610	2.0298	28	1.7404	3.6695	2.1624	28	2.2402	5.3129	2.7094
29	5.0044	3.9729	4.4612	29	4.5084	2.0183	2.4110	29	3.4680	2.3800	1.7863	29	4.2917	4.2776	2.3843
30	5.3780	3.1136	2.8420	30	4.1425	2.5003	2.4518	30	4.2776	2.2160	1.8207	30	4.3656	3.1034	2.4200
31	3.3010	3.1212	1.8003	31	2.6278	3.9308	2.4327	31	3.8237	3.0817	3.4170	31	4.7392	2.9363	3.8225
32	2.6648	7.7852	3.4196	32	1.5440	7.0112	2.5436	32	1.9967	7.7354	3.2449	32	2.3027	6.3253	3.5522
33	2.9236	7.9331	4.3465	33	1.6626	6.9794	2.6635	33	1.9469	7.4766	3.0587	33	2.2427	7.8362	3.6567
34	2.7719	7.5314	4.7035	34	1.4191	5.8765	2.0362	34	1.9877	7.4001	2.7170	34	2.2070	7.9280	3.0473
35	4.9049	6.7358	5.4392	35	2.4544	4.6589	2.1038	35	1.6460	6.3597	2.2287	35	2.0234	7.6322	2.9631
36	5.7005	6.2883	4.9228	36	3.6784	3.2589	2.7642	36	2.8994	4.7392	1.7213	36	3.5547	6.9067	2.6405
37	5.4927	4.7290	3.0498	37	3.6274	2.9861	2.8037	37	4.1897	3.0434	2.4008	37	4.4077	5.3066	3.9563
38	4.9725	4.2343	3.5917	38	2.8165	3.6134	2.4837	38	4.0112	3.0906	2.9338	38	4.6448	4.2254	3.8594
39	3.8607	3.1429	3.1811	39	2.4378	4.1450	2.0183	39	3.6873	3.8505	2.3103	39	4.4013	3.2793	2.9682
40	2.8547	3.9818	2.7897	40	1.6996	3.2194	2.9185	40	1.9788	3.3354	2.7056	40	1.3949	3.9767	2.6240
41	2.6099	3.5050	4.0112	41	2.5857	2.7680	2.4059	41	3.4387	2.9185	2.3460	41	3.7307	3.6083	2.6711
42	2.5271	3.7166	3.6733	42	1.8794	5.5998	2.2529	42	2.6189	4.8616	2.7362	42	3.3405	3.4272	3.4412
43	3.7638	7.6283	4.5212	43	1.4612	7.5251	2.6252	43	1.8730	7.7278	3.1684	43	2.4773	6.2666	3.7727
44	3.6746	8.3347	5.2262	44	1.4140	7.4741	2.2784	44	1.4994	7.7711	2.9006	44	1.7672	8.2034	3.2615
45	5.1434	7.9254	5.4035	45	2.2823	6.5038	2.2249	45	1.5861	7.4205	1.9495	45	1.8526	8.1855	2.6380
46	5.6789	7.0890	4.1017	46	3.5152	4.7825	3.4106	46	3.0804	6.6568	1.8194	46	3.4400	8.0427	2.7846
47	5.9823	6.1761	3.8021	47	3.7115	3.2207	3.1709	47	3.8633	4.4727	3.4068	47	3.8875	6.6147	4.2662
48	5.7095	4.8272	3.6580	48	2.2746	3.1799	3.1314	48	3.6822	2.9988	3.9321	48	4.2266	4.4141	4.3337
49	4.9610	3.2538	3.5993	49	1.6065	4.0443	3.6848	49	3.1429	3.8888	3.9487	49	4.2368	3.6950	4.3707
50	4.4625	2.2721	3.4973	50	2.0464	3.5279	2.4353	50	2.7974	2.7489	2.6775	50	3.7128	2.3868	3.5407
51	3.5126	4.6729	4.1208	51	1.9431	5.9147	2.7808	51	2.2606	4.9075	3.2462	51	3.1148	4.0622	3.7957
52	4.4842	7.1196	4.8807	52	1.5721	7.3147	2.7515	52	2.0719	7.1005	3.1225	52	3.1378	5.5131	3.6835
53	4.2585	8.1434	5.2543	53	1.4331	7.9139	2.1254	53	1.5836	8.0631	2.8203	53	2.1509	7.3619	3.1378
54	5.3537	8.1230	4.9878	54	2.4977	7.2599	2.4952	54	1.7098	8.3054	1.8883	54	1.8832	8.0669	2.6482
55	5.9160	7.6615	3.7001	55	3.3533	6.2297	3.4565	55	2.8152	7.2688	2.2568	55	3.2895	8.0937	3.0995
56	6.1557	6.7001	3.4247	56	3.5573	4.2827	2.8892	56	3.4897	6.1736	3.6899	56	3.6746	7.1872	4.2891
57	5.9428	3.0932	3.1620	57	1.7557	3.2538	2.9325	57	3.3290	3.0651	3.5866	57	3.9053	2.9810	3.9143
58	4.6079	2.7833	4.4434	58	2.3626	4.8437	2.8586	58	3.2474	2.9376	3.3711	58	4.1489	2.6558	3.9104
59	4.8425	5.7031	4.8131	59	1.8386	7.0316	2.4812	59	2.4365	5.6891	3.1110	59	3.4808	5.0388	3.6389
60	5.2658	7.1502	4.9547	60	1.5657	7.8859	2.2491	60	1.7009	7.8349	2.4263	60	2.7005	6.7983	3.3647
61	5.8025	8.4099	4.3580	61	2.5577	7.7507	3.0230	61	1.8220	7.8438	1.8921	61	2.1344	7.9267	2.3830
62	6.0129	7.8158	3.1021	62	3.1505	7.2573	3.4629	62	2.8445	7.9292	2.4710	62	3.0549	8.1842	3.1850
63	6.4286	7.2662	2.7578	63	3.3380	5.6967	2.7502	63	3.1913	6.9105	3.5955	63	3.5624	7.4741	3.8594
64	6.2207	5.0745	2.4939	64	2.2249	3.2156	2.4646	64	3.3635	3.9755	3.4489	64	3.7498	4.9827	3.7115
65	4.8654	7.1821	4.3478	65	2.2759	7.1974	2.6992	65	2.4531	7.3555	2.9720	65	2.8037	6.9755	3.8837
66	5.3869	5.3920	4.8144	66	2.6405	5.7375	2.2466	66	3.2768	5.7656	2.9083	66	4.5836	5.6291	3.7077
67	5.8650	7.1196	4.4243	67	1.9571	7.5251	2.9414	67	2.0872	6.7562	2.0553	67	2.9848	6.5165	2.4429
68	6.1787	7.8999	3.4706	68	3.0906	7.4116	3.3431	68	2.6240	7.6666	2.7770	68	2.6686	8.0593	3.0651
69	6.3839	7.3453	3.7523	69	3.1926	6.4566	2.9096	69	3.2870	7.0967	3.4017	69	3.3660	7.5965	3.5432
70	6.2909	5.4073	3.1569	70	2.6928	4.3758	2.6890	70	3.1199	4.9776	3.0014	70	3.7090	5.4876	2.9006
71	5.8204	3.4591	2.7782	71	1.7659	3.1709	2.1713	71	2.9657	2.9912	2.4518	71	3.8875	3.0893	2.5194
72	5.1370	6.6428	4.3350	72	2.9096	6.7269	2.4225	72	3.0664	6.7881	2.8088	72	4.0214	6.8455	3.6950
73	4.9674	4.7864	3.3902	73	3.3698	4.3733	2.4939	73	4.0915	4.5479	2.9440	73	4.5645	4.2738	3.6414
74	5.7005	6.													

Hayward Field 2-2-07 - Uped_{F5} Values [m/s] (cont'd)

conversion 1.7

Uref_{F5} = 7.5 m/s

Upper Speed Limit = 2 [m/s]
Lower Speed Limit = 1.5 [m/s]

Existing				90 degrees to the wind				75 degrees to the wind				60 degrees to the wind			
#	N	NW	NE	#	N	NW	NE	#	N	NW	NE	#	N	NW	NE
81	5.4557	3.8097	3.7842	81	4.4039	3.6287	2.6393	81	5.1880	3.5993	2.7795	81	5.6342	3.5981	3.5432
82	5.7936	5.4685	3.8569	82	3.6044	5.4328	2.3269	82	4.1336	5.6776	2.8930	82	5.0171	5.4647	3.2296
83	6.1965	6.0983	4.1412	83	3.2194	6.2807	2.9083	83	3.7409	6.0129	2.4786	83	4.5071	6.0397	3.1697
84	6.3151	4.9126	5.9810	84	2.7566	5.5195	5.5386	84	3.0294	4.9623	3.8225	84	4.2955	4.9534	3.7039
85	6.4898	6.7601	6.7728	85	3.5636	6.9016	6.2271	85	3.4948	6.7741	5.9632	85	3.5483	6.7907	5.3780
86	6.6479	7.0597	5.4494	86	3.5713	6.8697	4.9062	86	3.4476	6.9539	5.3933	86	3.9614	7.0610	5.5552
87	6.5038	5.9415	3.6937	87	3.6962	5.1459	3.3482	87	3.1939	6.1098	3.4948	87	3.6618	5.9479	3.7421
88	6.2131	5.1752	3.0562	88	4.3286	4.5441	2.7489	88	2.9733	4.9317	2.9937	88	3.5267	5.2339	3.1633
89	5.4392	3.2130	4.2050	89	4.7953	2.8433	3.0243	89	5.9772	2.9019	3.0919	89	6.1787	2.9924	3.5993
90	5.9428	4.0902	4.0660	90	4.3529	4.0877	2.7884	90	5.0694	3.6975	2.8063	90	5.6623	3.8888	3.2411
91	6.0843	4.4306	6.3329	91	3.4820	4.8680	6.0665	91	4.1310	4.6385	5.3219	91	4.7685	4.7366	4.1514
92	6.3839	5.3078	7.4078	92	3.5420	5.5985	7.2012	92	3.5713	5.0643	6.8863	92	4.0800	4.9585	6.2819
93	6.5752	6.8136	5.6228	93	4.0048	6.5089	4.9751	93	3.9614	6.4732	5.5373	93	4.4714	6.6198	5.7860
94	6.6032	5.5220	3.3533	94	4.6206	5.5463	2.9861	94	3.2666	5.5399	3.2207	94	3.8862	5.8051	3.3278
95	6.0856	3.2321	5.7898	95	5.0197	3.0026	5.3448	95	5.6381	3.1671	4.1297	95	6.1736	3.0600	3.6771
96	6.6185	4.7481	7.4855	96	3.8429	4.7876	7.3440	96	4.3401	4.6448	7.2790	96	5.0962	5.1204	6.2029
97	6.5905	5.1191	7.1260	97	3.7103	5.1319	6.7894	97	3.7421	5.2466	6.8531	97	4.4931	5.2632	6.6925
98	6.6848	6.2768	5.4596	98	4.2266	6.2169	4.5530	98	4.2419	5.7617	5.0375	98	4.6448	5.7974	5.5463
99	6.4898	6.4426	3.1671	99	5.1905	6.3737	2.9147	99	3.6644	6.1455	3.1097	99	4.0354	6.4196	3.4565
100	5.9135	6.2309	6.3376	100	5.1383	6.2577	2.9465	100	3.4578	6.2335	3.4578	100	3.8327	6.4120	3.5611
101	5.7821	2.9478	6.2998	101	5.1587	2.9198	6.8493	101	5.8739	2.7285	5.9747	101	6.6746	2.8981	4.8297
102	5.4022	3.1595	7.9280	102	4.3299	3.4591	7.9981	102	5.2224	3.3558	7.2777	102	5.8357	3.4145	6.6083
103	5.6470	3.3214	6.9105	103	4.4281	3.0422	6.7537	103	5.5730	3.0638	6.4171	103	6.2156	3.3890	6.1085
104	6.0002	4.0749	7.1196	104	4.5161	3.8480	7.0801	104	5.5820	3.7829	6.9845	104	6.1532	4.0940	6.5663
105	6.2131	5.7426	7.1987	105	3.8569	6.1009	7.0967	105	4.4842	6.0550	6.8595	105	5.3015	6.2628	7.4396
106	6.3865	6.6198	6.3419	106	3.9818	6.7932	6.5000	106	3.7944	6.5153	6.4706	106	4.7188	6.7256	6.6874
107	6.3954	6.1417	4.9088	107	4.5569	6.0843	4.1272	107	4.4995	6.0588	4.6321	107	4.6691	6.2526	4.8539
108	6.4222	6.3444	3.1811	108	5.4978	6.2348	2.7056	108	4.0647	6.1889	2.9006	108	4.5569	6.5357	3.1837
109	5.3882	3.7319	5.7566	109	3.9729	4.0035	5.9581	109	4.9776	3.8148	5.6330	109	5.4825	3.8824	5.8854
110	6.2743	5.7617	6.8021	110	3.9780	5.8408	6.3980	110	4.7443	5.5220	6.4528	110	5.7018	5.7133	6.4298
111	6.3278	6.0894	3.5738	111	4.5518	5.8892	3.1824	111	4.1514	6.0741	3.2207	111	4.5390	6.4120	6.8236
112	6.0703	6.4464	2.3690	112	5.3690	6.5675	2.2019	112	3.7574	6.3317	2.0145	112	4.1425	6.4910	2.5092
113	5.5271	5.8217	5.9810	113	3.8072	5.8038	5.4124	113	4.3988	5.6049	5.4902	113	5.0809	5.9173	5.7299
114	5.8752	6.7945	6.1481	114	3.8021	6.6861	5.7707	114	4.1973	7.0355	5.7783	114	4.9700	7.0444	6.0575
115	5.1497	6.3470	4.7813	115	3.7957	6.3291	3.9946	115	3.5636	6.7014	4.1654	115	3.9385	6.5905	4.5428
116	5.9530	6.7830	4.6079	116	4.3490	6.7333	3.9653	116	4.0175	6.8442	4.3184	116	4.4600	7.0826	4.4957
117	5.2020	6.0741	3.3915	117	4.1986	5.5386	2.7400	117	3.7549	6.2399	2.9618	117	4.0316	6.4426	3.4030
118	5.4060	6.7511	2.0668	118	4.7124	6.4222	2.4021	118	3.8913	6.6619	2.0260	118	3.8582	6.8723	1.9112
119	3.8503	4.5263	3.7664	119	4.7532	5.5820	5.1803	119	4.2254	7.0482	4.0698	119	4.1680	7.6985	3.5254
120	3.8263	2.6010	6.0996	120	4.0494	2.6890	5.8140	120	4.0673	2.6482	5.3448	120	4.8399	2.6010	5.4863
121	3.4374	4.6436		121	5.2849	6.0448		121	5.2466	6.3329		121	4.5734	7.4116	
122	2.7209	4.5403		122	4.9062	3.3456		122	5.2951	3.5381		122	5.6036	3.9933	

Existing 90 degrees to the wind

Profiles at 40 ft height (full scale)		Profiles at 50 ft height (full scale)	
#	N	#	N
35	8.5973	35	3.8964
45	8.5731	45	3.9449
54	8.5310	54	4.0226
61	8.5234	61	4.5135
67	8.5476	67	4.3452
76	8.5833	76	4.7558
84	8.5451	84	5.1752
92	8.4074	92	6.0269
97	8.2748	97	6.4337
106	8.4762	106	6.4171

Profiles at 50 ft height (full scale)		Profiles at 60 ft height (full scale)	
#	N	#	N
35	9.4286	35	6.1022
45	8.9135	45	6.2118
54	9.0270	54	6.4337
61	8.8562	61	6.9577
67	8.9480	67	6.3023
76	9.1494	76	6.8812
84	8.8982	84	7.3121
92	9.1392	92	7.5518
97	8.6764	97	7.9662
106	8.7312	106	7.8145

Profiles at 60 ft height (full scale)	
#	N
35	9.3636
45	9.4796
54	9.5536
61	9.3164
67	9.4159
76	9.4694
84	9.4567
92	9.0971
97	9.1507
106	8.9378

Hayward Field 2-2-07 - Turbulent Intensity Values [%]

Existing				90 degrees to the wind				75 degrees to the wind				60 degrees to the wind			
#	N	NW	NE	#	N	NW	NE	#	N	NW	NE	#	N	NW	NE
1	45.86	33.48	47.66	1	28.61	49.73	47.41	1	35.47	40.70	50.15	1	42.51	38.77	46.69
2	53.15	32.63	54.58	2	21.16	41.07	34.01	2	26.88	39.10	30.58	2	33.60	33.23	40.11
3	50.79	34.42	50.43	3	21.95	37.07	30.03	3	26.40	35.00	27.62	3	28.24	30.08	32.70
4	45.21	38.79	46.71	4	23.71	32.80	26.08	4	27.02	32.66	25.78	4	28.11	29.26	26.89
5	51.00	35.60	38.40	5	26.77	36.45	38.27	5	32.63	32.37	36.80	5	34.26	29.69	36.34
6	39.25	39.75	33.55	6	32.25	32.39	46.87	6	41.03	33.10	45.15	6	43.71	28.76	39.38
7	57.56	33.86	45.52	7	37.31	31.22	50.30	7	42.62	31.03	51.96	7	52.44	29.92	51.45
8	52.25	32.78	40.10	8	32.41	32.08	52.41	8	36.17	31.95	51.55	8	45.11	33.42	46.83
9	44.68	29.39	42.00	9	35.31	31.13	51.74	9	38.59	33.03	48.64	9	43.60	31.30	47.48
10	46.99	34.23	37.36	10	27.59	45.14	42.39	10	29.25	43.55	45.09	10	32.26	36.01	37.14
11	50.43	33.57	35.44	11	30.50	46.52	45.07	11	33.86	40.82	43.06	11	37.37	37.06	40.17
12	47.57	34.83	54.08	12	22.32	48.35	32.79	12	22.88	39.99	35.95	12	25.15	29.89	42.00
13	33.00	39.87	31.18	13	41.46	52.34	44.14	13	40.25	60.06	44.15	13	37.06	58.22	41.49
14	53.95	33.11	42.84	14	59.21	35.28	52.80	14	55.55	35.73	51.34	14	59.25	32.54	44.92
15	41.56	45.53	52.75	15	47.49	51.64	52.07	15	48.82	51.12	51.90	15	45.87	45.25	50.74
16	69.50	44.99	22.57	16	59.58	34.37	21.59	16	62.17	38.04	21.00	16	54.39	38.79	22.92
17	34.46	48.61	49.60	17	45.69	53.83	54.68	17	51.68	56.64	52.97	17	48.34	59.33	47.10
18	52.20	62.04	48.85	18	55.94	47.05	55.23	18	54.74	50.16	46.74	18	61.42	41.55	50.39
19	45.14	54.64	20.75	19	30.60	60.16	20.36	19	36.06	51.72	22.34	19	38.67	40.28	23.09
20	45.23	37.86	50.58	20	36.24	45.56	43.16	20	41.96	40.39	43.29	20	47.50	40.85	43.28
21	46.06	42.26	36.17	21	60.77	54.74	50.69	21	43.79	51.07	56.62	21	43.72	41.01	62.05
22	43.89	46.98	34.66	22	59.10	54.71	57.34	22	59.34	51.90	58.41	22	60.80	45.34	58.73
23	51.44	55.36	48.83	23	52.23	51.36	40.03	23	44.78	51.14	42.23	23	40.36	37.04	44.84
24	46.34	56.14	48.40	24	51.72	47.67	38.95	24	56.09	52.08	41.57	24	55.11	50.37	40.16
25	39.90	42.68	51.02	25	42.23	52.05	46.70	25	39.79	41.66	48.73	25	41.10	51.56	45.70
26	49.73	42.48	48.69	26	40.44	50.40	54.81	26	37.57	42.72	56.83	26	39.80	39.01	56.35
27	54.55	42.44	36.43	27	61.52	60.45	55.55	27	42.67	45.37	54.02	27	46.40	34.14	53.75
28	37.71	44.94	31.38	28	53.87	60.66	60.65	28	48.40	49.05	58.25	28	42.17	40.05	56.66
29	33.01	46.91	39.32	29	43.57	55.65	52.66	29	55.24	46.39	51.41	29	53.12	42.76	48.83
30	35.53	50.82	48.92	30	47.10	56.88	53.87	30	39.46	44.13	52.11	30	41.70	46.81	50.32
31	49.56	54.19	53.08	31	48.86	45.92	50.97	31	33.69	44.09	54.26	31	33.13	40.35	55.90
32	50.75	44.08	49.87	32	46.43	33.53	49.57	32	46.72	33.58	47.10	32	40.09	54.28	44.18
33	51.94	32.62	44.39	33	53.66	38.07	48.32	33	45.41	28.50	46.80	33	39.83	46.18	42.59
34	49.43	28.89	33.37	34	51.40	47.28	54.12	34	44.64	33.48	50.34	34	39.57	30.14	45.46
35	36.85	30.85	30.85	35	47.26	51.81	59.05	35	46.05	38.43	56.85	35	50.19	29.27	51.83
36	31.33	37.80	37.62	36	35.95	59.36	54.95	36	47.40	46.12	56.70	36	51.45	33.20	51.31
37	28.80	47.74	51.67	37	37.35	52.50	47.59	37	33.57	45.96	55.41	37	32.34	46.34	41.51
38	40.11	53.06	35.49	38	52.65	47.46	52.27	38	31.57	42.12	45.45	38	25.25	43.75	38.60
39	47.01	43.77	43.15	39	50.73	45.17	48.32	39	34.57	43.39	45.87	39	31.30	37.99	43.49
40	41.90	34.45	28.75	40	39.37	45.96	20.51	40	48.96	41.85	21.70	40	44.07	39.59	24.12
41	45.64	46.64	41.47	41	43.81	40.98	48.52	41	38.94	49.25	48.98	41	37.10	42.05	48.88
42	55.45	48.43	50.11	42	59.48	40.61	45.82	42	54.06	45.98	53.61	42	47.05	40.55	46.01
43	53.14	46.55	41.45	43	55.41	29.86	55.58	43	46.78	34.19	48.06	43	43.19	49.97	38.45
44	43.18	28.21	32.99	44	55.38	35.51	57.62	44	45.28	28.29	45.12	44	44.13	37.47	40.08
45	31.33	25.60	32.54	45	48.65	44.48	56.26	45	56.58	34.23	53.86	45	54.81	28.42	48.99
46	26.84	28.54	39.86	46	33.14	54.29	49.94	46	45.65	40.36	60.71	46	49.28	29.73	46.05
47	27.89	38.83	41.19	47	33.60	54.75	45.50	47	31.01	50.83	45.32	47	34.14	40.49	34.57
48	28.32	49.60	39.26	48	46.99	46.87	39.51	48	29.48	44.14	30.43	48	24.34	46.75	27.28
49	35.99	42.18	37.29	49	42.94	49.11	34.67	49	45.23	43.44	27.45	49	31.05	39.46	28.82
50	45.11	54.59	42.48	50	63.31	47.20	56.34	50	56.17	51.69	56.31	50	54.29	54.15	45.54
51	54.35	50.31	47.35	51	55.07	38.20	56.22	51	42.89	46.04	52.55	51	42.77	48.90	43.23
52	44.61	43.50	37.86	52	57.78	28.68	63.06	52	52.24	37.36	46.29	52	44.67	43.77	39.09
53	34.82	33.59	32.22	53	57.98	29.95	57.39	53	54.49	30.55	46.43	53	48.72	38.73	40.31
54	27.07	25.50	38.35	54	43.95	37.60	56.53	54	57.17	31.64	55.88	54	56.43	33.26	56.36
55	26.01	27.49	45.18	55	31.57	50.21	43.23	55	46.09	38.40	62.60	55	46.15	29.62	45.23
56	26.52	33.30	49.63	56	37.49	57.73	44.07	56	29.11	49.58	41.40	56	35.00	36.68	33.67
57	27.56	50.17	38.83	57	66.28	49.10	31.48	57	32.78	48.98	28.03	57	24.44	44.31	28.75
58	39.38	56.19	41.55	58	59.62	47.59	60.52	58	56.30	48.31	54.85	58	48.82	50.83	43.04
59	35.62	43.53	36.06	59	57.54	31.84	61.75	59	51.94	41.05	55.12	59	43.99	46.32	39.32
60	31.79	32.08	36.09	60	62.19	27.75	58.67	60	53.80	29.68	53.88	60	44.72	36.68	47.10
61	27.49	28.52	44.35	61	47.19	31.25	49.22	61	63.03	28.97	60.46	61	59.61	32.97	52.41
62	24.51	25.28	50.96	62	34.66	46.40	44.09	62	48.36	33.96	60.57	62	50.59	27.42	45.19
63	23.52	30.09	61.15	63	39.92	56.35	49.50	63	30.26	42.15	42.78	63	33.60	33.64	34.26
64	26.30	47.68	33.85	64	50.50	53.68	34.57	64	29.60	54.30	32.11	64	26.80	48.64	31.79
65	33.88	30.14	48.17	65	37.90	28.93	55.99	65	38.87	30.24	55.05	65	38.38	26.01	43.41
66	31.12	41.86	41.19	66	51.63	33.07	61.51	66	48.11	40.51	56.98	66	40.15	42.87	43.99
67	27.47	35.67	49.27	67	60.32	29.85	53.49	67	58.15	32.84	57.89	67	46.21	38.35	52.31
68	23.07	27.64	61.85	68	41.70	34.85	48.11	68	51.54	29.33	49.83	68	52.20	31.06	42.04
69	24.21	29.79	54.67	69	43.07	43.68	55.28	69	31.87	37.08	45.41	69	35.64	32.19	40.39
70	26.79	41.74	32.24	70	55.23	53.69	29.63	70	29.66	48.71	33.56	70	26.14	43.80	32.53
71	27.00	52.90	29.25	71	52.36	57.26	24.35	71	34.26	53.07	25.33	71	24.60	51.61	28.34
72	29.02	35.32	46.69	72	49.57	33.72	54.12	72	51.28	34.14	52.03	72	42.46	33.43	46.76
73	34.41	43.84	51.57	73	46.87	45.26	49.03	73	41.35	48.85	51.46	73	36.99	44.95	45.05
74	28.35	35.10</													

Hayward Field 2-2-07 - Turbulent Intensity Values [%] (cont'd)

Existing				90 degrees to the wind				75 degrees to the wind				60 degrees to the wind			
#	N	NW	NE	#	N	NW	NE	#	N	NW	NE	#	N	NW	NE
81	28.22	35.91	44.97	81	35.56	37.37	48.06	81	32.64	36.35	43.30	81	28.72	34.23	39.29
82	29.52	37.87	47.68	82	47.20	33.83	49.11	82	38.45	38.11	49.06	82	36.49	37.74	43.79
83	27.09	41.91	50.00	83	50.66	38.76	59.99	83	40.85	41.90	66.89	83	37.64	43.20	52.79
84	24.16	41.55	42.52	84	57.31	36.84	45.30	84	49.13	42.32	60.29	84	38.30	43.46	60.29
85	22.96	34.72	30.50	85	51.58	33.91	33.28	85	55.74	37.81	40.40	85	46.42	40.21	41.30
86	23.11	29.38	35.21	86	46.35	33.12	36.29	86	40.73	31.16	35.89	86	38.27	32.54	38.75
87	25.44	33.08	30.20	87	46.65	44.39	28.57	87	31.60	38.26	31.37	87	29.91	38.59	32.29
88	24.90	36.61	28.59	88	41.91	43.69	28.27	88	31.80	42.01	27.87	88	24.60	36.81	26.94
89	24.50	29.24	38.38	89	34.21	29.65	44.18	89	29.83	28.50	44.08	89	24.36	27.24	32.82
90	26.85	35.93	44.28	90	37.79	35.14	49.60	90	30.98	34.90	48.84	90	27.33	34.34	42.26
91	24.98	49.73	41.42	91	53.34	45.62	42.40	91	42.41	48.28	61.33	91	32.08	50.03	62.16
92	21.69	41.97	27.44	92	53.52	41.29	29.91	92	52.26	44.56	34.95	92	38.34	44.37	44.19
93	22.42	31.68	34.13	93	45.95	33.48	33.86	93	43.88	36.93	34.71	93	43.17	36.29	33.74
94	23.04	29.61	29.58	94	39.31	38.18	27.84	94	32.22	34.42	28.15	94	28.72	32.75	26.41
95	25.94	30.93	40.74	95	36.89	30.64	45.68	95	30.04	30.13	54.90	95	25.29	28.80	44.40
96	25.12	47.69	28.58	96	56.78	47.62	29.77	96	38.74	47.20	37.75	96	33.44	48.40	48.26
97	23.53	40.79	25.84	97	49.06	41.50	26.92	97	50.20	45.82	28.23	97	37.97	42.87	31.61
98	23.22	34.34	31.87	98	49.43	37.12	32.28	98	45.63	39.36	33.37	98	43.06	36.92	31.21
99	21.47	27.41	30.07	99	38.23	31.02	31.63	99	33.87	29.23	31.51	99	29.85	28.05	27.37
100	21.36	22.73	33.10	100	38.72	25.72	45.22	100	30.58	24.83	41.62	100	28.42	23.50	30.75
101	23.22	29.58	30.33	101	35.72	32.08	34.19	101	28.17	30.15	42.07	101	25.05	29.69	38.42
102	28.85	42.69	27.15	102	37.97	45.71	25.87	102	33.10	45.28	30.06	102	28.35	43.77	32.90
103	31.56	36.43	29.97	103	46.52	36.83	29.23	103	38.29	35.47	36.63	103	31.40	35.37	44.13
104	26.85	36.20	27.53	104	46.90	37.99	28.22	104	35.97	35.66	33.99	104	33.14	34.45	44.16
105	26.92	41.75	26.60	105	50.33	41.13	25.53	105	42.59	40.44	30.20	105	34.62	36.93	33.31
106	25.15	37.36	27.86	106	58.14	41.65	31.06	106	49.54	40.69	31.27	106	40.30	38.80	30.19
107	23.68	35.11	32.42	107	47.79	33.73	33.92	107	52.59	35.29	34.92	107	45.17	35.65	33.13
108	24.81	29.84	31.96	108	43.83	31.00	38.39	108	41.92	31.57	38.87	108	40.78	32.05	30.45
109	34.52	38.70	31.93	109	47.31	40.90	34.87	109	46.01	37.43	37.28	109	36.46	37.56	40.19
110	28.41	38.53	28.35	110	49.04	40.94	30.05	110	41.42	40.45	31.59	110	36.00	39.26	33.31
111	28.48	34.22	33.26	111	48.14	32.77	34.29	111	53.62	33.81	32.93	111	47.75	34.20	31.40
112	26.01	29.54	42.36	112	47.02	29.98	40.22	112	46.45	29.84	39.46	112	37.20	27.45	39.28
113	29.78	40.15	33.91	113	48.57	40.94	37.96	113	40.13	42.21	37.09	113	35.04	39.26	35.20
114	27.87	35.32	29.99	114	49.89	39.08	35.42	114	47.07	38.49	35.44	114	38.55	36.10	32.79
115	35.33	38.18	38.40	115	51.33	40.63	40.04	115	55.20	42.86	39.72	115	46.50	40.28	37.17
116	30.26	37.11	35.22	116	51.11	37.85	37.54	116	49.78	41.89	37.16	116	47.51	37.13	34.07
117	34.22	37.87	35.58	117	48.44	39.46	36.26	117	53.67	37.71	34.65	117	48.29	39.93	34.02
118	25.49	19.02	38.04	118	37.58	20.31	31.58	118	38.20	20.65	35.72	118	34.53	19.77	36.37
119	48.46	32.66	41.25	119	33.13	51.98	42.19	119	39.62	43.01	43.18	119	43.40	33.27	45.60
120	38.09	38.73	21.71	120	35.00	40.93	28.41	120	37.18	38.23	30.44	120	33.81	36.96	27.60
121	43.96	33.38	0.00	121	27.62	46.34	0.00	121	32.50	45.58	0.00	121	35.64	36.37	0.00
122	37.33	41.24	0.00	122	34.12	45.37	0.00	122	32.20	46.21	0.00	122	32.39	44.45	0.00

Existing 90 degrees to the wind

Profiles at 40 ft height (full scale)

#	N	#	N
35	25.65	35	37.09
45	25.10	45	36.57
54	24.74	54	36.03
61	22.78	61	34.37
67	24.42	67	44.84
76	23.07	76	44.69
84	22.68	84	47.35
92	20.84	92	40.25
97	19.66	97	41.07
106	20.85	106	38.50

Profiles at 50 ft height (full scale)

#	N	#	N
35	21.32	35	36.41
45	22.56	45	37.16
54	21.66	54	34.59
61	20.11	61	35.27
67	21.54	67	40.93
76	21.01	76	40.77
84	19.97	84	42.50
92	20.33	92	35.44
97	19.25	97	40.92
106	20.06	106	39.41

Profiles at 60 ft height (full scale)

#	N	#	N
35	18.68	35	38.09
45	17.67	45	36.19
54	19.84	54	35.83
61	19.16	61	36.99
67	20.21	67	38.90
76	16.99	76	40.33
84	20.91	84	38.43
92	19.44	92	34.19
97	18.01	97	34.90
106	19.51	106	36.86

Hayward Field 2-2-07 - R Values

Existing				90 degrees to the wind				75 degrees to the wind				60 degrees to the wind			
#	N	NW	NE	#	N	NW	NE	#	N	NW	NE	#	N	NW	NE
1	0.2461	0.3419	0.2083	1	0.3782	0.4790	0.3635	1	0.3432	0.5456	0.2868	1	0.3035	0.5861	0.2647
2	0.2819	0.3524	0.2095	2	0.4497	0.4681	0.4237	2	0.3939	0.5180	0.3848	2	0.3701	0.5470	0.3262
3	0.2577	0.3467	0.1916	3	0.4181	0.4625	0.4490	3	0.3416	0.4935	0.4372	3	0.3317	0.5060	0.3836
4	0.3219	0.3570	0.2819	4	0.3769	0.4943	0.4932	4	0.3300	0.5203	0.4870	4	0.3350	0.4958	0.4508
5	0.2420	0.3130	0.3413	5	0.3492	0.5069	0.5760	5	0.3397	0.5041	0.5470	5	0.3558	0.4827	0.5471
6	0.4469	0.2833	0.4608	6	0.3538	0.4622	0.4101	6	0.3398	0.5117	0.3979	6	0.3403	0.4636	0.4401
7	0.2663	0.3657	0.5226	7	0.3930	0.4244	0.5119	7	0.3277	0.4486	0.5017	7	0.3220	0.4420	0.5373
8	0.2849	0.3770	0.3870	8	0.4381	0.4253	0.3863	8	0.3710	0.4354	0.3564	8	0.3759	0.4590	0.3740
9	0.2383	0.3877	0.4028	9	0.3560	0.4345	0.3398	9	0.3039	0.4564	0.3813	9	0.2940	0.4465	0.4063
10	0.4772	0.3250	0.4614	10	0.4887	0.3547	0.4122	10	0.4375	0.3657	0.3871	10	0.4450	0.3621	0.4021
11	0.4350	0.3638	0.3838	11	0.4738	0.3784	0.3885	11	0.4358	0.3989	0.3565	11	0.4322	0.3961	0.3735
12	0.3859	0.3417	0.3385	12	0.6294	0.3602	0.4041	12	0.5778	0.3530	0.3711	12	0.5514	0.3518	0.3683
13	0.2805	0.4031	0.2282	13	0.3027	0.3627	0.1871	13	0.3290	0.3076	0.1965	13	0.3797	0.2724	0.2114
14	0.1937	0.1912	0.2033	14	0.1939	0.1404	0.2051	14	0.1993	0.1428	0.2017	14	0.2458	0.1467	0.1885
15	0.2747	0.1227	0.3130	15	0.2537	0.1069	0.3107	15	0.2575	0.1088	0.3064	15	0.2544	0.1086	0.3043
16	0.2204	0.4292	0.4940	16	0.1807	0.4499	0.4999	16	0.2049	0.4450	0.4830	16	0.2293	0.4387	0.4791
17	0.1693	0.1341	0.1505	17	0.2258	0.0969	0.1130	17	0.1630	0.1009	0.1247	17	0.1721	0.1114	0.1259
18	0.3275	0.2078	0.2407	18	0.2665	0.1732	0.1832	18	0.2523	0.1491	0.1566	18	0.2842	0.1297	0.1940
19	0.1659	0.1990	0.2461	19	0.2378	0.2274	0.2757	19	0.2172	0.2269	0.2810	19	0.1955	0.1610	0.2740
20	0.2040	0.2149	0.1847	20	0.1965	0.1126	0.2987	20	0.1753	0.1520	0.3101	20	0.1495	0.1955	0.3656
21	0.1478	0.2191	0.2904	21	0.1676	0.1124	0.1223	21	0.1659	0.1518	0.1530	21	0.1788	0.2269	0.2395
22	0.3657	0.2135	0.3766	22	0.2724	0.1443	0.1961	22	0.1870	0.1253	0.1858	22	0.2776	0.2114	0.2050
23	0.3193	0.2212	0.1448	23	0.2445	0.2512	0.1654	23	0.3512	0.2263	0.1621	23	0.4426	0.1653	0.2565
24	0.1753	0.3029	0.1849	24	0.1308	0.3445	0.1200	24	0.1306	0.3481	0.1232	24	0.1607	0.2603	0.1363
25	0.1750	0.5637	0.1964	25	0.1420	0.3820	0.1927	25	0.1700	0.4704	0.2221	25	0.1948	0.4801	0.2349
26	0.2597	0.3219	0.2661	26	0.1538	0.2196	0.2333	26	0.1831	0.2948	0.2429	26	0.1899	0.3995	0.2791
27	0.2030	0.3723	0.3381	27	0.1738	0.2374	0.1463	27	0.1630	0.3494	0.1682	27	0.1908	0.4636	0.2252
28	0.3740	0.3574	0.3910	28	0.1999	0.1538	0.1592	28	0.1365	0.2878	0.1696	28	0.1757	0.4167	0.2125
29	0.3925	0.3116	0.3499	29	0.3536	0.1583	0.1891	29	0.2720	0.1869	0.1401	29	0.3366	0.3355	0.1870
30	0.4218	0.2442	0.2229	30	0.3249	0.1961	0.1923	30	0.3355	0.1738	0.1428	30	0.3424	0.2434	0.1898
31	0.2589	0.2448	0.1412	31	0.2061	0.3083	0.1908	31	0.2999	0.2417	0.2680	31	0.3717	0.2303	0.2998
32	0.2090	0.6106	0.2682	32	0.1211	0.5499	0.1995	32	0.1566	0.6067	0.2545	32	0.1806	0.4961	0.2786
33	0.2293	0.6222	0.3409	33	0.1304	0.5474	0.2089	33	0.1527	0.5864	0.2399	33	0.1759	0.6146	0.2868
34	0.2174	0.5907	0.3689	34	0.1113	0.4609	0.1597	34	0.1559	0.5804	0.2131	34	0.1731	0.6218	0.2390
35	0.3847	0.5283	0.4266	35	0.1925	0.3654	0.1650	35	0.1291	0.4988	0.1748	35	0.1587	0.5986	0.2324
36	0.4471	0.4932	0.3861	36	0.2885	0.2556	0.2168	36	0.2274	0.3717	0.1350	36	0.2788	0.5417	0.2071
37	0.4308	0.3709	0.2392	37	0.2845	0.2342	0.2199	37	0.3286	0.2387	0.1883	37	0.3457	0.4162	0.3103
38	0.3900	0.3321	0.2817	38	0.2209	0.2834	0.1948	38	0.3146	0.2424	0.2301	38	0.3643	0.3314	0.3027
39	0.3028	0.2465	0.2495	39	0.1912	0.3251	0.1583	39	0.2892	0.3020	0.1812	39	0.3452	0.2572	0.2328
40	0.2239	0.3123	0.2188	40	0.1333	0.2525	0.2289	40	0.1552	0.2616	0.2122	40	0.1094	0.3119	0.2058
41	0.2047	0.2749	0.3146	41	0.2028	0.2171	0.1887	41	0.2697	0.2289	0.1840	41	0.2926	0.2830	0.2095
42	0.1982	0.2915	0.2881	42	0.1474	0.4392	0.1767	42	0.2054	0.3813	0.2146	42	0.2620	0.2688	0.2699
43	0.2952	0.5983	0.3546	43	0.1146	0.5902	0.2059	43	0.1469	0.6061	0.2485	43	0.1943	0.4915	0.2959
44	0.2882	0.6537	0.4099	44	0.1109	0.5862	0.1787	44	0.1176	0.6095	0.2275	44	0.1386	0.6434	0.2558
45	0.4034	0.6216	0.4238	45	0.1790	0.5101	0.1745	45	0.1244	0.5820	0.1529	45	0.1453	0.6420	0.2069
46	0.4454	0.5560	0.3217	46	0.2757	0.3751	0.2675	46	0.2416	0.5221	0.1427	46	0.2698	0.6308	0.2184
47	0.4692	0.4844	0.2982	47	0.2911	0.2526	0.2487	47	0.3030	0.3508	0.2672	47	0.3049	0.5188	0.3346
48	0.4478	0.3786	0.2869	48	0.1784	0.2494	0.2456	48	0.2888	0.2352	0.3084	48	0.3315	0.3462	0.3399
49	0.3891	0.2552	0.2823	49	0.1260	0.3172	0.2890	49	0.2465	0.3050	0.3097	49	0.3323	0.2898	0.3428
50	0.3500	0.1782	0.2743	50	0.1605	0.2767	0.1910	50	0.2194	0.2156	0.2100	50	0.2912	0.1872	0.2777
51	0.2755	0.3665	0.3232	51	0.1524	0.4639	0.2181	51	0.1773	0.3849	0.2546	51	0.2443	0.3186	0.2977
52	0.3517	0.5584	0.3828	52	0.1233	0.5737	0.2158	52	0.1625	0.5569	0.2449	52	0.2461	0.4324	0.2889
53	0.3340	0.6387	0.4121	53	0.1124	0.6207	0.1687	53	0.1242	0.6324	0.2212	53	0.1687	0.5774	0.2461
54	0.4199	0.6371	0.3912	54	0.1959	0.5694	0.1957	54	0.1341	0.6514	0.1481	54	0.1477	0.6327	0.2077
55	0.4640	0.6009	0.2902	55	0.2630	0.4886	0.2711	55	0.2208	0.5701	0.1770	55	0.2580	0.6348	0.2431
56	0.4828	0.5255	0.2686	56	0.2790	0.3359	0.2266	56	0.2737	0.4842	0.2894	56	0.2882	0.5637	0.3364
57	0.4661	0.2426	0.2480	57	0.1377	0.2552	0.2300	57	0.2611	0.2404	0.2813	57	0.3063	0.2338	0.3070
58	0.3614	0.2183	0.3485	58	0.1853	0.3799	0.2242	58	0.2547	0.2304	0.2644	58	0.3254	0.2083	0.3067
59	0.3798	0.4473	0.3775	59	0.1442	0.5515	0.1946	59	0.1911	0.4462	0.2440	59	0.2730	0.3952	0.2854
60	0.4130	0.5608	0.3886	60	0.1228	0.6185	0.1764	60	0.1334	0.6145	0.1903	60	0.2118	0.5332	0.2639
61	0.4551	0.6596	0.3418	61	0.2006	0.6079	0.2371	61	0.1429	0.6152	0.1484	61	0.1674	0.6217	0.1869
62	0.4716	0.6130	0.2433	62	0.2471	0.5692	0.2716	62	0.2231	0.6219	0.1938	62	0.2396	0.6419	0.2498
63	0.5042	0.5699	0.2163	63	0.2618	0.4468	0.2157	63	0.2503	0.5420	0.2820	63	0.2794	0.5862	0.3027
64	0.4879	0.3980	0.1956	64	0.1745	0.2522	0.1933	64	0.2638	0.3118	0.2705	64	0.2941	0.3908	0.2911
65	0.3816	0.5633	0.3410	65	0.1785	0.5645	0.2117	65	0.1924	0.5769	0.2331	65	0.2199	0.5471	0.3046
66	0.4225	0.4229	0.3776	66	0.2071	0.4500	0.1762	66	0.2570	0.4522	0.2281	66	0.3595	0.4415	0.2908
67	0.4600	0.5584	0.3470	67	0.1535	0.5902	0.2307	67	0.1637	0.5299	0.1612	67	0.2341	0.5111	0.1916
68	0.4846	0.6196	0.2722	68	0.2424	0.5813	0.2622	68	0.2058	0.6013	0.2178	68	0.2093	0.6321	0.2404
69	0.5007	0.5761	0.2943	69	0.2504	0.5064	0.2282	69	0.2578	0.5566	0.2668	69	0.2640	0.5958	0.2779
70	0.4934	0.4241	0.2476	70	0.2112	0.3432	0.2109	70	0.2447	0.3904	0.2354	70	0.2909	0.4304	0.2275
71	0.4565	0.2713	0.2179	71	0.1385	0.2487	0.1703	71	0.2326	0.2346	0.1923	71	0.3049	0.2423	0.1976
72	0.4029	0.5210	0.3												

Hayward Field 2-2-07 - R Values (cont'd)

Existing				90 degrees to the wind				75 degrees to the wind				60 degrees to the wind			
#	N	NW	NE	#	N	NW	NE	#	N	NW	NE	#	N	NW	NE
81	0.4279	0.2988	0.2968	81	0.3454	0.2846	0.2070	81	0.4069	0.2823	0.2180	81	0.4419	0.2822	0.2779
82	0.4544	0.4289	0.3025	82	0.2827	0.4261	0.1825	82	0.3242	0.4453	0.2269	82	0.3935	0.4286	0.2533
83	0.4860	0.4783	0.3248	83	0.2525	0.4926	0.2281	83	0.2934	0.4716	0.1944	83	0.3535	0.4737	0.2486
84	0.4953	0.3853	0.4691	84	0.2162	0.4329	0.4344	84	0.2376	0.3892	0.2998	84	0.3369	0.3885	0.2905
85	0.5090	0.5302	0.5312	85	0.2795	0.5413	0.4884	85	0.2741	0.5313	0.4677	85	0.2783	0.5326	0.4218
86	0.5214	0.5537	0.4274	86	0.2801	0.5388	0.3848	86	0.2704	0.5454	0.4230	86	0.3107	0.5538	0.4357
87	0.5101	0.4660	0.2897	87	0.2899	0.4036	0.2626	87	0.2505	0.4792	0.2741	87	0.2872	0.4665	0.2935
88	0.4873	0.4059	0.2397	88	0.3395	0.3564	0.2156	88	0.2332	0.3868	0.2348	88	0.2766	0.4105	0.2481
89	0.4266	0.2520	0.3298	89	0.3761	0.2230	0.2372	89	0.4688	0.2276	0.2425	89	0.4846	0.2347	0.2823
90	0.4661	0.3208	0.3189	90	0.3414	0.3206	0.2187	90	0.3976	0.2900	0.2201	90	0.4441	0.3050	0.2542
91	0.4772	0.3475	0.4967	91	0.2731	0.3818	0.4758	91	0.3240	0.3638	0.4174	91	0.3740	0.3715	0.3256
92	0.5007	0.4163	0.5810	92	0.2778	0.4391	0.5648	92	0.2801	0.3972	0.5401	92	0.3200	0.3889	0.4927
93	0.5157	0.5344	0.4410	93	0.3141	0.5105	0.3902	93	0.3107	0.5077	0.4343	93	0.3507	0.5192	0.4538
94	0.5179	0.4331	0.2630	94	0.3624	0.4350	0.2342	94	0.2562	0.4345	0.2526	94	0.3048	0.4553	0.2610
95	0.4773	0.2535	0.4541	95	0.3937	0.2355	0.4192	95	0.4422	0.2484	0.3239	95	0.4842	0.2400	0.2884
96	0.5191	0.3724	0.5871	96	0.3014	0.3755	0.5760	96	0.3404	0.3643	0.5709	96	0.3997	0.4016	0.4865
97	0.5169	0.4015	0.5589	97	0.2910	0.4025	0.5325	97	0.2935	0.4115	0.5375	97	0.3524	0.4128	0.5249
98	0.5243	0.4923	0.4282	98	0.3315	0.4876	0.3571	98	0.3327	0.4519	0.3951	98	0.3643	0.4547	0.4350
99	0.5090	0.5053	0.2484	99	0.4071	0.4999	0.2286	99	0.2874	0.4820	0.2439	99	0.3165	0.5035	0.2711
100	0.4638	0.4887	0.2853	100	0.4030	0.4908	0.2311	100	0.2712	0.4889	0.2712	100	0.3006	0.5029	0.2793
101	0.4535	0.2312	0.4941	101	0.4046	0.2290	0.5372	101	0.4607	0.2140	0.4686	101	0.5235	0.2273	0.3788
102	0.4237	0.2478	0.6218	102	0.3396	0.2713	0.6273	102	0.4096	0.2632	0.5708	102	0.4577	0.2678	0.5183
103	0.4429	0.2605	0.5420	103	0.3473	0.2386	0.5297	103	0.4371	0.2403	0.5033	103	0.4875	0.2658	0.4791
104	0.4706	0.3196	0.5584	104	0.3542	0.3018	0.5553	104	0.4378	0.2967	0.5478	104	0.4826	0.3211	0.5150
105	0.4873	0.4504	0.5646	105	0.3025	0.4785	0.5566	105	0.3517	0.4749	0.5380	105	0.4158	0.4912	0.5835
106	0.5009	0.5192	0.4974	106	0.3123	0.5328	0.5098	106	0.2976	0.5110	0.5075	106	0.3701	0.5275	0.5245
107	0.5016	0.4817	0.3850	107	0.3574	0.4772	0.3237	107	0.3529	0.4752	0.3633	107	0.3662	0.4904	0.3807
108	0.5037	0.4976	0.2495	108	0.4312	0.4890	0.2122	108	0.3188	0.4854	0.2275	108	0.3574	0.5126	0.2497
109	0.4226	0.2927	0.4515	109	0.3116	0.3140	0.4673	109	0.3904	0.2992	0.4418	109	0.4300	0.3045	0.4616
110	0.4921	0.4519	0.5335	110	0.3120	0.4581	0.5018	110	0.3721	0.4331	0.5061	110	0.4472	0.4481	0.5043
111	0.4963	0.4776	0.2803	111	0.3570	0.4619	0.2496	111	0.3256	0.4764	0.2526	111	0.3560	0.5029	0.2842
112	0.4761	0.5056	0.1858	112	0.4211	0.5151	0.1727	112	0.2947	0.4966	0.1580	112	0.3249	0.5091	0.1968
113	0.4335	0.4566	0.4691	113	0.2986	0.4552	0.4245	113	0.3450	0.4396	0.4306	113	0.3985	0.4641	0.4494
114	0.4608	0.5329	0.4822	114	0.2982	0.5244	0.4526	114	0.3292	0.5518	0.4532	114	0.3898	0.5525	0.4751
115	0.4039	0.4978	0.3750	115	0.2977	0.4964	0.3133	115	0.2795	0.5256	0.3267	115	0.3089	0.5169	0.3563
116	0.4669	0.5320	0.3614	116	0.3411	0.5281	0.3110	116	0.3151	0.5368	0.3387	116	0.3498	0.5555	0.3526
117	0.4080	0.4764	0.2660	117	0.3293	0.4344	0.2149	117	0.2945	0.4894	0.2323	117	0.3162	0.5053	0.2669
118	0.4240	0.5295	0.1621	118	0.3696	0.5037	0.1884	118	0.3052	0.5225	0.1589	118	0.3026	0.5390	0.1499
119	0.2863	0.3550	0.2954	119	0.3728	0.4378	0.4063	119	0.3314	0.5528	0.3192	119	0.3269	0.6038	0.2765
120	0.3001	0.2040	0.4784	120	0.3176	0.2109	0.4560	120	0.3190	0.2077	0.4192	120	0.3796	0.2040	0.4303
121	0.2696	0.3642	0.0000	121	0.4145	0.4741	0.0000	121	0.4115	0.4967	0.0000	121	0.3587	0.5813	0.0000
122	0.2134	0.3561	0.0000	122	0.3848	0.2624	0.0000	122	0.4153	0.2775	0.0000	122	0.4395	0.3132	0.0000

Existing 90 degrees to the wind

Profiles at 40 ft height (full scale)		90 degrees to the wind	
#	N	#	N
35	0.6743	35	0.3056
45	0.6724	45	0.3094
54	0.6691	54	0.3155
61	0.6685	61	0.3540
67	0.6704	67	0.3408
76	0.6732	76	0.3730
84	0.6702	84	0.4059
92	0.6594	92	0.4727
97	0.6490	97	0.5046
106	0.6648	106	0.5033

Profiles at 50 ft height (full scale)

Profiles at 50 ft height (full scale)		90 degrees to the wind	
#	N	#	N
35	0.7395	35	0.3568
45	0.6991	45	0.3683
54	0.7080	54	0.3966
61	0.6946	61	0.4317
67	0.7018	67	0.4163
76	0.7176	76	0.4611
84	0.6979	84	0.4692
92	0.7168	92	0.5543
97	0.6805	97	0.5739
106	0.6848	106	0.5605

Profiles at 60 ft height (full scale)

Profiles at 60 ft height (full scale)		90 degrees to the wind	
#	N	#	N
35	0.7344	35	0.4786
45	0.7435	45	0.4872
54	0.7493	54	0.5046
61	0.7307	61	0.5457
67	0.7385	67	0.4943
76	0.7427	76	0.5397
84	0.7417	84	0.5735
92	0.7135	92	0.5923
97	0.7177	97	0.6248
106	0.7010	106	0.6129

APPENDIX B. THE ATMOSPHERIC BOUNDARY LAYER WIND TUNNEL

In the present investigation, the Atmospheric Boundary Layer Wind Tunnel (ABLWT) located at University of California, Davis (UC Davis) was used (Figure B-1). Built in the 1980's, the wind tunnel was originally designed to simulate turbulent boundary layers comparable to wind flow near the surface of the earth. In order to achieve this effect, the tunnel requires a long flow-development section such that a mature boundary-layer flow is produced at the test section. The wind tunnel is an open-return type with an overall length of 21.3 m and is composed of five sections: the entrance, the flow-development section, the test section, the diffuser section, and the fan and motor.

The entrance section is elliptical in shape with a smooth contraction area that minimizes the free-stream turbulence of the incoming flow. Following the contraction area is a commercially available air filter that reduces large-scale pressure fluctuations of the flow and filters larger-size particles out of the incoming flow. Behind the filter, a honeycomb flow straightener is used to reduce large-scale turbulence.

The flow development section is 12.2 m long with an adjustable ceiling for longitudinal pressure-gradient control. For the present study, the ceiling was diverged ceiling so that a zero-pressure-gradient condition is formed in the stream wise direction. At the leading edge of the section immediately following the honeycomb flow straightener, four triangularly shaped spires are stationed on the wind-tunnel floor to provide favorable turbulent characteristics in the boundary-layer flow. Roughness elements are then placed all over the floor of this section to artificially thicken the boundary layer. For a free-stream wind speed of 4.0 m/s, the wind-tunnel boundary layer grows to a height of one meter at the test section. With a thick boundary layer, larger models could be tested and thus measurements could be made at higher resolution.

Dimensions of the test section are 2.44 m in stream wise length, 1.66 m high, and 1.18 m wide. Similar to the flow-development section, the test section ceiling can also be adjusted to obtain the desired stream wise pressure gradient. Experiments can be observed from both sides of the

test section through framed Plexiglas® windows. One of the windows is also a sliding door that allows access into the test section. When closed twelve clamps distributed over the top and lower edges are used to seal the door. Inside the test section, a three-dimensional probe-positioning system is installed at the ceiling to provide fast and accurate sensor placement. The traversing system scissor-type extensions, which provide vertical probe motion, are also made of aerodynamically shaped struts to minimize flow disturbances.

The diffuser section is 2.37 m long and has an expansion area that provides a continuous transition from the rectangular cross-section of the test section to the circular cross-sectional area of the fan. To eliminate upstream swirl effects from the fan and avoid flow separation in the diffuser section, fiberboard and honeycomb flow straighteners are placed between the fan and diffuser sections.

The fan consists of eight constant-pitch blades 1.83 m in diameter and is powered by a 56 kW (75 hp) variable-speed DC motor. A dual belt and pulley drive system is used to couple the motor and the fan.

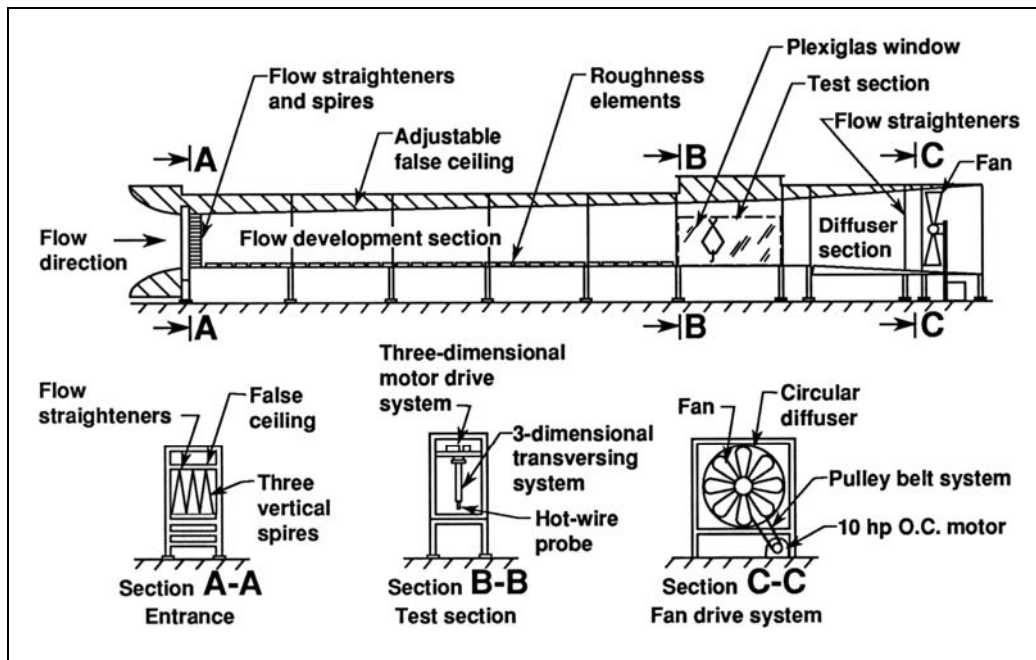


Figure B-1. Schematic diagram of the UC Davis Atmospheric Boundary Layer Wind Tunnel.

APPENDIX C. WIND-TUNNEL ATMOSPHERIC FLOW SIMILARITY PARAMETERS

Wind-tunnel models of a particular test site are typically several orders of magnitude smaller than the full-scale size. In order to appropriately simulate atmospheric winds in the UC Davis Atmospheric Boundary Layer Wind Tunnel (ABLWT), certain flow parameters must be satisfied between a model and its corresponding full-scale equivalent. Similitude parameters can be obtained by non-dimensionalizing the equations of motion, which build the starting point for the similarity analysis. Fluid motion can be described by the following time-averaged equations.

Conservation of mass:

$$\frac{\partial \bar{U}_i}{\partial t_i} = 0 \quad \text{and} \quad \frac{\partial \rho}{\partial t} + \frac{\partial(\rho \bar{U}_i)}{\partial x_i} = 0$$

Conservation of momentum:

$$\frac{\partial \bar{U}_i}{\partial t} + \bar{u}_i \frac{\partial \bar{U}_i}{\partial x_j} + 2\varepsilon_{ijk} \Omega_j \bar{U}_k = -\frac{1}{\rho_0} \frac{\partial \delta P}{\partial x_i} - \frac{\delta T}{T_0} g \delta_{i3} + \nu_0 \frac{\partial^2 \bar{U}_i}{\partial x_j^2} + \frac{\partial(-\overline{u_j u_i})}{\partial x_j}$$

Conservation of energy:

$$\frac{\partial \delta \bar{T}}{\partial t} + \bar{U}_i \frac{\partial \delta \bar{T}}{\partial x_i} = \left[\frac{\kappa_0}{\rho_0 c_{p_0}} \right] \frac{\partial^2 \delta \bar{T}}{\partial x_k \partial x_k} + \frac{\partial(-\overline{\theta u_i})}{\partial x_i} + \frac{\bar{\phi}}{\rho_0 c_{p_0}}$$

Here, the mean quantities are represented by capital letters while the fluctuating values by small letters. δP is the deviation of pressure in a neutral atmosphere. ρ_0 and T_0 are the density and temperature of a neutral atmosphere and ν_0 is the kinematic viscosity. In the equation for the conservation of energy, ϕ is the dissipation function, $\delta \bar{T}$ is the deviation of temperature from the temperature of a neutral atmosphere, κ_0 is the thermal diffusivity, and c_{p_0} is the heat capacity.

Applying the Boussinesq density approximation, application of the equations is then restricted to fluid flows where $\delta \bar{T} \ll T_0$.

Defining the following non-dimensional quantities and then substituting into the above equations yields:

$$\begin{aligned}\bar{U}'_i &= \bar{U}_i / U_0; \quad u'_i = u_i / U_0; \quad x'_i = x_i / L_0; \quad t' = tU_0 / L_0; \quad \Omega'_j = \Omega_j / \Omega_0; \quad \bar{\delta P}' = \bar{\delta P} / \rho_0 U_0^2; \\ \bar{\delta T}' &= \bar{\delta T} / \delta T_0; \quad g' = g / g_0; \quad \bar{\varphi}' = \bar{\varphi} / \varphi_0\end{aligned}$$

The equations of motion can be presented in the following dimensionless forms.

Continuity Equation:

$$\frac{\partial u'_i}{\partial x'_i} = 0 \quad \text{and} \quad \frac{\partial \rho'}{\partial t'} + \frac{\partial(\rho' u'_i)}{\partial x'_i} = 0$$

Momentum Equation:

$$\frac{\partial \bar{U}'_i}{\partial t'} + \bar{U}'_j \frac{\partial \bar{U}'_i}{\partial x'_j} + \frac{2}{\text{Ro}} \varepsilon_{ijk} \bar{U}'_k \Omega'_j = -\frac{\partial \bar{\delta P}'}{\partial x'_i} + \frac{1}{\text{Fr}^2} \bar{\delta T}' \delta_{3i} + \frac{1}{\text{Re}} \frac{\partial^2 \bar{U}'_i}{\partial x'_j \partial x'_j} + \frac{\partial(-\bar{u}'_j \bar{u}'_i)}{\partial x'_j}$$

Turbulent Energy Equation:

$$\frac{\partial \bar{\delta T}'}{\partial t'} + \bar{U}'_i \frac{\partial \bar{\delta T}'}{\partial x'_i} = \text{Pr} \cdot \frac{1}{\text{Re}} \frac{\partial^2 \bar{\delta T}'}{\partial x'_k \partial x'_k} + \frac{\partial(-\bar{\theta}' u'_i)}{\partial x'_i} + \frac{1}{\text{Re}} \cdot \text{Ec} \cdot \bar{\varphi}'$$

Although the continuity equation gives no similarity parameters, coefficients from both other equations do provide the following desired similarity parameters.

Rosby number:
$$\text{Ro} \equiv U_0 / L_0 \Omega_0$$

Densimetric Froude number:
$$\text{Fr} \equiv U_0 / (gL_0 \delta T_0 / T_0)^{1/2}$$

Prandtl number:
$$\text{Pr} \equiv \rho_0 c_{p_0} \nu_0 / \kappa_0$$

Eckert number:
$$Ec \equiv \frac{U_0^2}{c_{p_0} \delta T_0}$$

Reynolds number:
$$Re \equiv \frac{U_0 L_0}{\nu_0}$$

In the dimensionless momentum equation, the Rossby number is extracted from the denominator of the third term on the left hand side. The Rossby number represents the ratio of advective acceleration to Coriolis acceleration due to the rotation of the earth. If the Rossby number is large, Coriolis accelerations are small. Since UC Davis ABLWT is not rotating, the Rossby number is infinite allowing the corresponding term in the dimensionless momentum equation to approach zero. In nature, however, the rotation of the earth influences the upper layers of the atmosphere; thus, the Rossby number is small and becomes important to match, and the corresponding term in the momentum equation is sustained.

Most modelers have assumed the Rossby number to be large, thus, neglecting the respective term in the equations of motion and ignoring the Rossby number as a criterion for modeling. Snyder (1972) showed that the characteristic length scale, L_0 , must be smaller than 5 km in order to simulate diffusion under neutral or stable conditions in relatively flat terrain. Other researchers discovered similar findings. Since UC Davis ABLWT produces a boundary layer with a height of about one meter, the surface layer vertically extends 10 to 15 cm above the ground. In this region the velocity spectrum would be accurately modeled. The Rossby number can then be ignored in this region. Since testing is limited to the lower 10% to 15% of the boundary layer, the length in longitudinal direction, which can be modeled, has to be no more than a few kilometers. Derived from the denominator of the second term on the right hand side of the dimensionless momentum equation, the square of the Froude number represents the ratio of inertial forces to buoyancy forces. High values of the Froude number infer that the inertial forces are dominant. For values equal or less than unity, thermal effects become important. Since the conditions inside the UC Davis ABLWT are inherently isothermal, the wind tunnel generates a neutrally stable boundary layer; hence, the Froude number is infinitely large allowing the respective term in the momentum equation to approach zero.

The third parameter is the Prandtl number, which is automatically matched between the wind-tunnel flow and full-scale winds if the same fluid is been used. The Eckert number criterion is important only in compressible flow, which is not of interest for a low-speed wind tunnel.

Reynolds number represents the ratio of inertial to viscous forces. The reduced scale of a wind tunnel model results in a Reynolds number several orders of magnitude smaller than in full scale. Thus, viscous forces are more dominant in the model than in nature. No atmospheric flow could be modeled, if strict adherence to the Reynolds number criterion was required. However, several arguments have been made to justify the use of a smaller Reynolds number in a model. These arguments include laminar flow analogy, Reynolds number independence, and dissipation scaling. With the absence of thermal and Coriolis effects, several test results have shown that the scaled model flow will be dynamically similar to the full-scale case if a critical Reynolds number is larger than a minimum independence value. The gross structure of turbulence is similar over a wide range of Reynolds numbers. Nearly all modelers use this approach today.

Reference

Snyder, W. H., 1972 “Similarity criteria for the application of fluid models to the study of air pollution meteorology,” *Boundary-Layer Meteorology*, Vol. 3, pp113-134.

APPENDIX D. WIND-TUNNEL ATMOSPHERIC BOUNDARY-LAYER SIMILARITY

Wind-tunnel simulation of the atmospheric boundary layer under neutrally stable conditions must also meet non-dimensional boundary-layer similarity parameters between the scaled-model flow and its full-scale counterpart. The most important conditions are:

- The normalized mean velocity, turbulence intensity, and turbulent energy profiles.
- The roughness Reynolds number, $Re_z = z_0 u_* / \nu$.
- Jensen's length-scale criterion of z_0/H .
- The ratio of H/δ for H greater than $H/\delta > 0.2$.
- In the turbulent core of a neutrally stable atmospheric boundary layer, the relationship between the local flow velocity, U , versus its corresponding height, z , may be represented by the following velocity-profile equation.

$$\frac{U}{U_\infty} = \left(\frac{z}{\delta} \right)^\alpha$$

Here, U_∞ is the mean velocity of the inviscid flow above the boundary layer, δ is the height of the boundary layer, and α is the power-law exponent, which represents the upwind surface conditions. Wind-tunnel flow can be shaped such that the exponent α will closely match its corresponding full-scale value, which can be determined from field measurements of the local winds. The required power-law exponent, α , can then be obtained by choosing the appropriate type and distribution of roughness elements over the wind tunnel flow-development section.

Full-scale wind data suggest that the atmospheric wind profile at the site yields a nominal value of $\alpha = 0.2$. This condition was closely matched in the UC Davis Atmospheric Boundary Layer Wind Tunnel by systematically arranging a pattern of 2" x 4" wooden blocks of 9" in length along the upwind half of the flow-development section, and 1" x 4" wooden blocks in lengths of 5" along the downwind half of the flow-development section. The pattern generally consisted of

alternating sets of four and five blocks in one row for the larger blocks, then four blocks in a row (each row being slightly offset from the last) for the small blocks. A typical velocity profile is presented in Figure D-1, where the simulated power-law exponent is $\alpha = 0.2$.

In the lower 20% of the boundary layer height, the flow is then governed by a rough-wall or “law-of-the-wall” logarithmic velocity profile.

$$\frac{U}{u_*} = \frac{1}{\kappa} \ln\left(\frac{z}{z_o}\right)$$

Here, u_* is the surface friction velocity, κ is von Karman’s constant, and z_o is the roughness height. This region of the atmospheric boundary layer is relatively unaffected by the Coriolis force, the only region that can be modeled accurately by the wind tunnel (i.e., the lowest 100 m of the atmospheric boundary layer under neutral stability conditions). Thus, it is desirable to have the scaled-model buildings and its surroundings contained within this layer.

The geometric scale of the model should be determined by the size of the wind tunnel, the roughness height, z_o , and the power-law index, α . With a boundary-layer height of 0.6 m in the test section, the surface layer would be 0.15 m deep for the UC Davis ABLWT. For the current study, a majority of the model is contained in this region of full-scale similarity.

Due to scaling effects, full-scale agreement of simulated boundary-layer profiles can only be attained in wind tunnels with long flow-development sections. For full-scale matching of the normalized mean velocity profile, an upwind fetch of approximately 10 to 25 boundary-layer heights can be easily constructed. To fully simulate the normalized turbulence intensity and energy spectra profiles, the flow-development section needs to be extended to about 50 and 100 to 500 times the boundary-layer height, respectively. These profiles must at least meet full-scale similarities in the surface layer region. However, with the addition of spires and other flow tripping devices, the flow development length can be reduced to less than 20 boundary layer heights for most engineering applications.

In the UC Davis Atmospheric Boundary Layer Wind Tunnel, the maximum values of turbulence intensity near the surface range from 35% to 40%, similar to that in full scale. Thus, the turbulent intensity profile, u'/u versus z , should agree reasonably with the full-scale, particularly in the region where testing is performed. Figure D-2 displays a typical turbulence intensity profile of the boundary layer in the ABLWT test section.

The second boundary-layer condition involves the roughness Reynolds number, Re_z . According to the Reynolds number independence criterion, it is attained when the roughness Reynolds number is defined as follows.

$$Re_z = \frac{u_* z_0}{\nu} \geq 2.5$$

Here, u_* is the friction speed, z_0 is the surface roughness length and ν is the kinematic viscosity. Re_z larger than 2.5 ensures that the flow is aerodynamically rough. Therefore, wind tunnels with a high enough roughness Reynolds numbers simulate full-scale aerodynamically rough flows exactly. To generate a rough surface in the wind tunnel, roughness elements are placed on the wind tunnel floor. The height of the elements must be larger than the height of the viscous sub-layer in order to trip the flow. The UC Davis ABLWT satisfies this condition, since the roughness Reynolds number is about 40, when the wind tunnel free stream velocity, U_∞ , is equal 3.8 m/s, the friction speed, u_* , is 0.24 m/s, and the roughness height, z_0 , is 0.0025 m. Thus, the flow setting satisfies the Re number independence criterion and dynamically simulates the flow.

The last condition for the boundary layer is the characteristic scale height to boundary layer ratio, H/δ . There are two possibilities for the value of the ratio. If $H/\delta \geq 0.2$, then the ratios must be matched. If $(H/\delta)_{F.S.} < 0.2$, then only the general inequality of $(H/\delta)_{W.T.} < 0.2$ must be met (F.S. stands for full-scale and W.T. stands for wind tunnel). Using the law-of-the-wall logarithmic profile equation, instead of the power-law velocity profile, this principle would constrain the physical model to the 15% to 20% of the wind tunnel boundary-layer height.

Along with these conditions, two other constraints have to be met. First, the mean stream wise pressure gradient in the wind tunnel must be zero. Even if high- and low-pressure systems drive atmospheric boundary layer flows, the magnitude of the pressure gradient in the flow direction is negligible compared to the dynamic pressure variation caused by the boundary layer. The other constraint is that the model should not take up more than 5% to 15% of the cross-sectional area at any down wind location. This assures that local flow acceleration affecting the stream wise pressure gradient will not distort the simulation flow.

Simulations in the UC Davis ABLWT were not capable of producing stable or unstable boundary layer flows. In fact, proper simulation of unstable boundary layer flows could be a disadvantage in any wind tunnel due to the artificial secondary flows generated by the heating that dominate and distort the longitudinal mean-flow properties, thus, invalidating the similitude criteria. However, this is not considered as a major constraint, since the winds that produce annual an average dispersion are sufficiently strong, such that for flow over a complex terrain, the primary source of turbulence is due to mechanical shear and not due to diurnal or heating and cooling effects in the atmosphere.

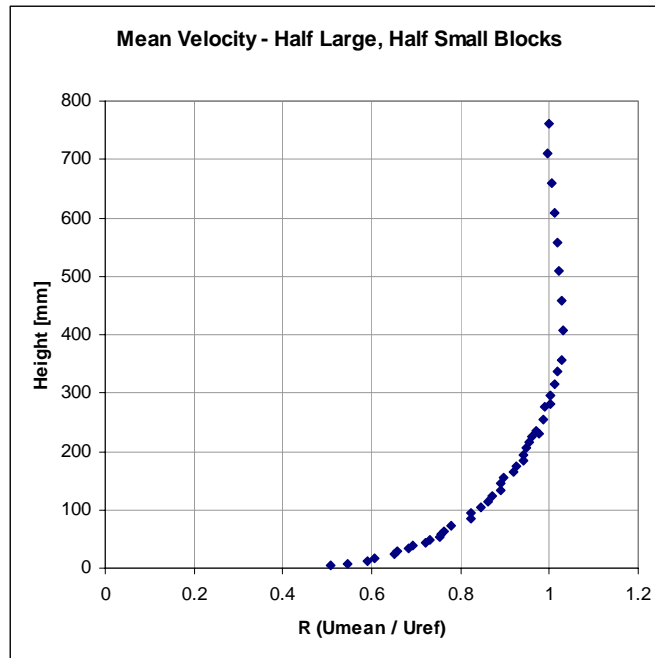


Figure D-1. Mean velocity profile in terms of R ($U_{\text{mean}}/U_{\text{ref}}$) for a typical wind direction in the wind tunnel. The power law exponent α is approximately 0.2. The reference velocity is 3.16 m/s.

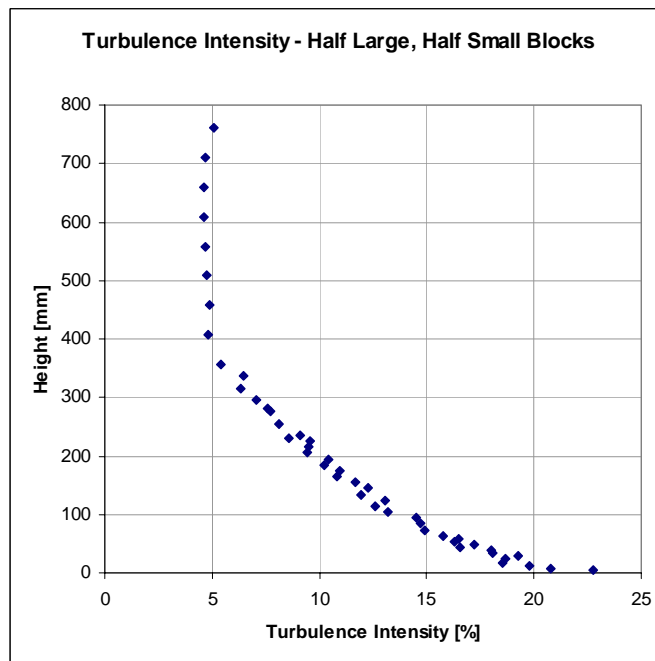


Figure D-2. Turbulence intensity profile corresponding to Figure D-1.